CHAPTER 3

EXPERIMENTAL RESULTS

3.1 Synthesis of Block Copolymers

3.1.1 Monomer Preparation

3.1.1.1 Synthesis of Glycolide

The synthesis of glycolide dates back to the early 1930s and the pioneering days of Carothers [19]. It is a two-step synthesis involving, firstly, the linear polycondensation of glycolic acid to low molecular weight poly(glycolic acid) ($\overline{M}_n < 5000$) followed, secondly, by thermal decomposition of the polymer to yield glycolide as the primary decomposition product, as shown below.

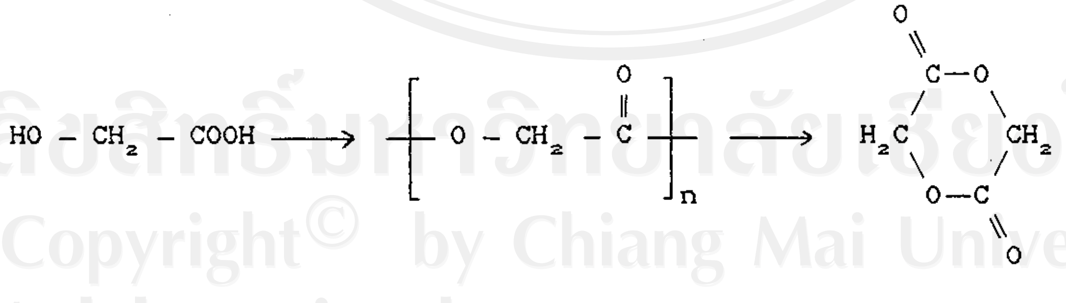

glycolic acid low mol. wt. PGA glycolide

In a typical synthesis reaction in this work, approximately 30 g of glycolic acid together with approximately 0.3 g of antimony trioxide catalyst (1% w/w) were heated at 120-130°C under a nitrogen atmosphere in a conventional short-path distillation apparatus (see Fig. 3.1a). Heating was continued for about 3 hours until the water of polycondensation ceased to distill from the flask. The apparatus was then adapted for vacuum take-off (see Fig. 3.1b) and heating continued for a further 1 hour at a reduced pressure of 2-4 mm Hg. Over the following 2 hours, the heating temperature was gradually increased up to 150°C and then, when the flask contents started to solidify, increased further up to 170°C. The product at this stage was low molecular weight poly(glycolic acid) (PGA). Finally, for an additional period of about 4 hours, the heating temperature was increased up to 270-285°C in order to thermally degrade the low molecular weight PGA to yield glycolide as the primary product. Crude glycolide began to distill out of the flask and solidify in the condenser at about 265°C. This crude product was obtained as a yellow crystalline solid in approximately 50-60% yield based on the initial glycolic acid. It had an observed melting range of 80-84°C (c.f., lit. [20] m.pt. 82-84°C).

The crude glycolide was stored in a vacuum desiccator until required for further use. It could be purified by recrystallisation from ethyl acetate at 50-60°C, the recrystallised material being a white, needle-like, crystalline solid of narrower melting range 82-84°C.

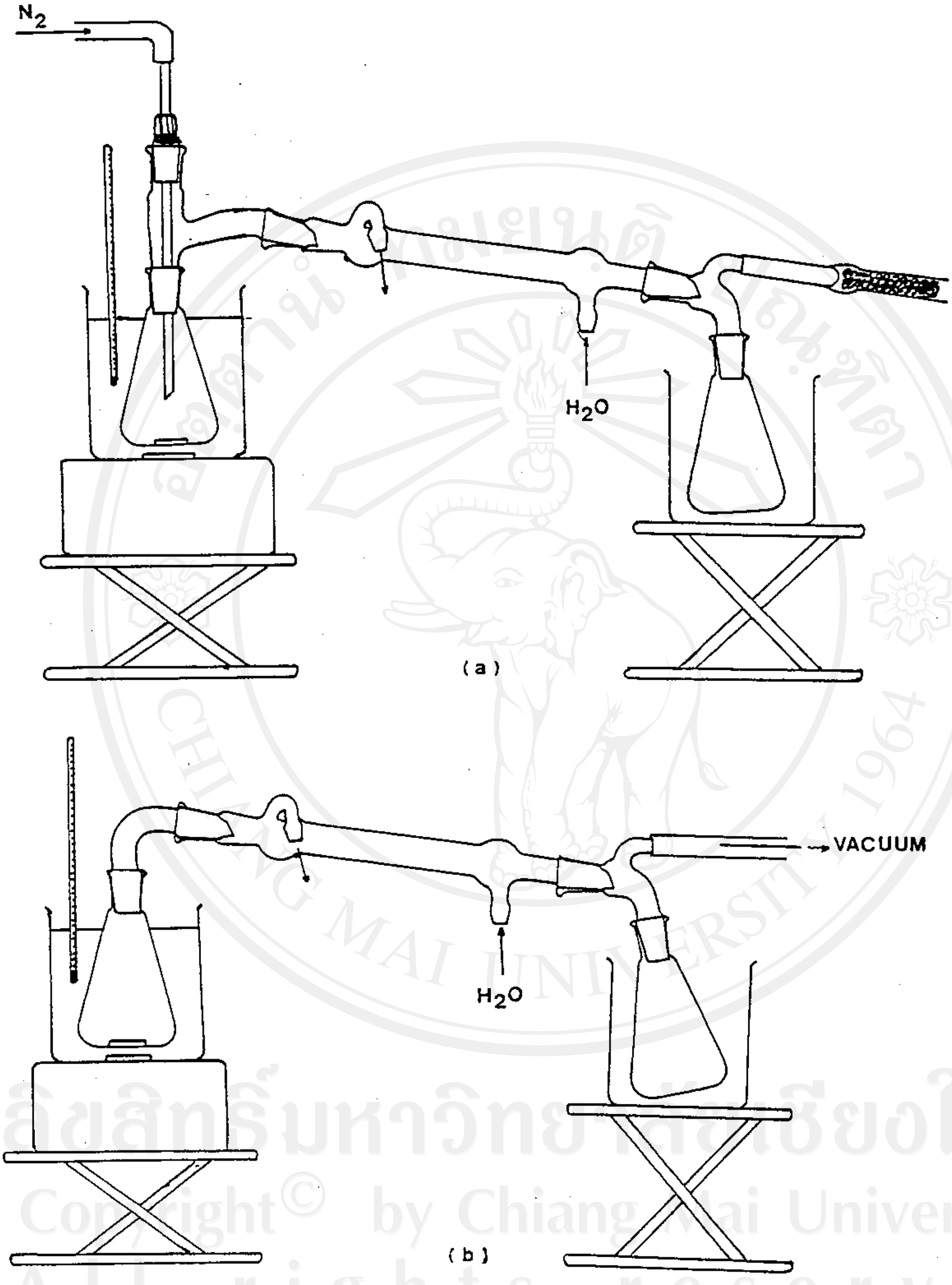

Fig. 3.1 : Apparatus used in the two-stage preparation of glycolide:
(a) glycolic acid polycondensation to low mol. wt. PGA
(b) thermal degradation of low mol. wt. PGA to glycolide

3.1.1.2 Purification of Poly(ethylene glycol)

Commercial poly(ethylene glycol) (PEG 200 and PEG 1500; $\overline{M}_n \simeq$ 190-210 and $\overline{M}_n \simeq$ 1500-1600; Fluka AG) was thoroughly dried before use by heating to 100 °C under vacuum with continuous magnetic stirring. Drying was considered to be complete when both constant weight and a constant O-H peak absorbance in the infrared spectrum were attained. Dried PEG was stored under vacuum to prevent contact with atmospheric moisture until required for use.

3.1.2 Synthesis of Poly(glycolic acid-b-oxyethylene)

In this work, the aim was to prepare a series of block copoly(ester-ether)s comprising poly(glycolic acid) segments attached to low molecular weight polyoxyethylene ($\overline{M}_n \simeq$ 200 and 1500) segments. The latter, more commonly referred to as poly(ethylene glycol) (PEG), is the "comonomer" with glycolide and forms the "soft" middle segment, as represented in the structure (II) below.

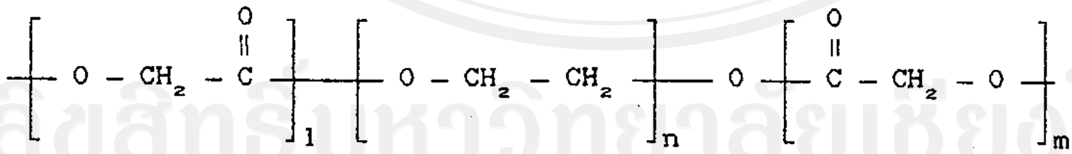

$$\left[O - CH_2 - \overset{\overset{O}{\|}}{C} \right]_l \left[O - CH_2 - CH_2 \right]_n O \left[\overset{\overset{O}{\|}}{C} - CH_2 - O \right]_m$$

ABA poly(glycolic acid-b-oxyethylene)

(II)

(a) Apparatus

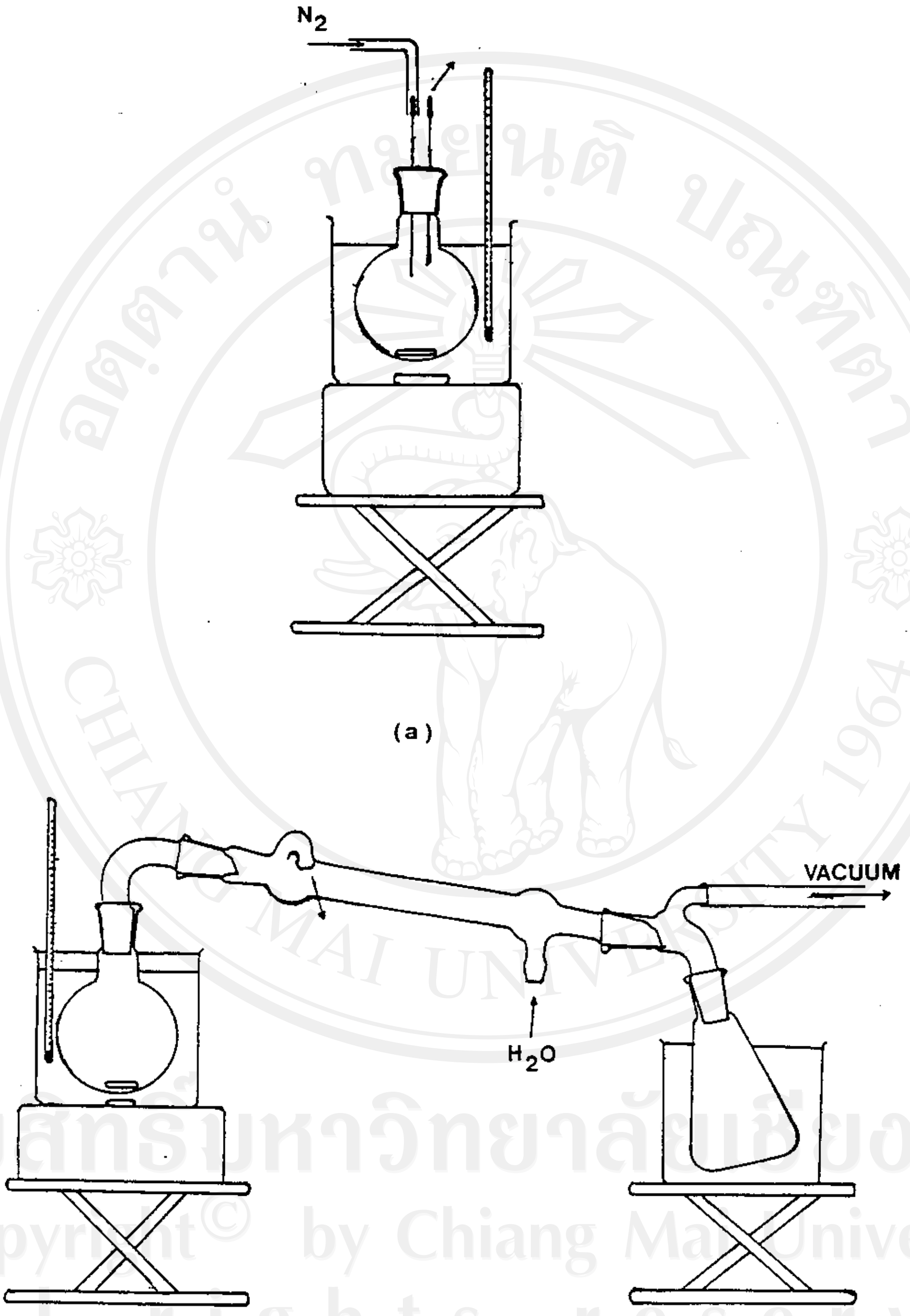

(a)

(b)

Fig. 3.2 : Apparatus used for the block copolymerisation of glycolide and PEG.

(b) Block Copolymerisation of Glycolide and Poly(ethylene glycol)

A series of experiments employing different PEG molecular weights, initiators, temperatures, and comonomer feed ratios were carried out, as summarized in Table 3.1. The two initiators used in this work were aluminium triethyl [used as a 10% v/v stock solution in disitilled decahydronaphthalene (decalin) as solvent] and stannous oxalate.

In a typical experiment, using the apparatus shown in Fig. 3.2a, approximately 5 g of glycolide and the appropriate weight of PEG (calculated as mole %) were mixed together under a dry nitrogen atmosphere at room temperature in a controlled atmosphere glove box. 1 mole % of the initiator was then added into the mixture and the reaction flask removed from the glove box. The mixture was immersed in an oil bath at the required temperature with stirring under a nitrogen atmosphere. After the system had been maintained under these conditions for 30 minutes, the pressure was gradually reduced to 3-4 mm Hg by connection to a vacuum pump (See Fig. 3.2b) and the reaction continued until the mixture had completely solidified. The crude product was obtained as a whitish solid with a slight brown discoloration.

The crude copolymer was stored in a vacuum desiccator until required for use. It could be purified by extraction with refluxing absolute ethanol, the purified copolymer being an off-white solid powder.

In this way, a series of copolymers with different compositions were prepared by varying the conditions of synthesis, as

Table 3.1 : Summary of polymerisation experiments carried out in this work.

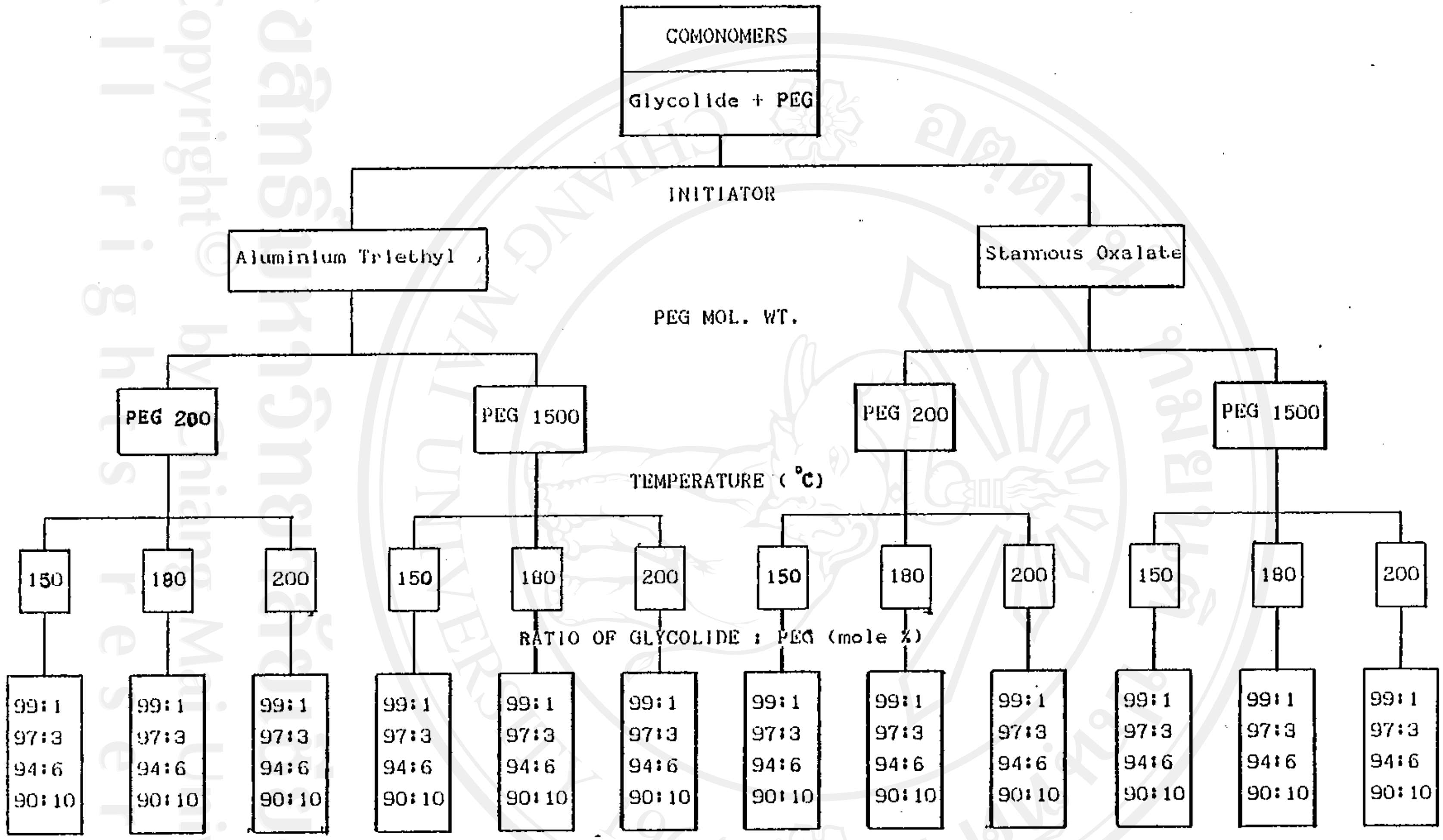

* $Al(C_2H_5)_3$ used as a 10% v/v solution in distilled decahydronaphthalene (decalin)

detailed in Table 3.1. The homopolymerisation of glycolide alone to poly(glycolic acid) was also carried out in a similar manner for comparison.

3.2 Purification of Poly(glycolic acid-b-oxyethylene) by Ethanol Extraction

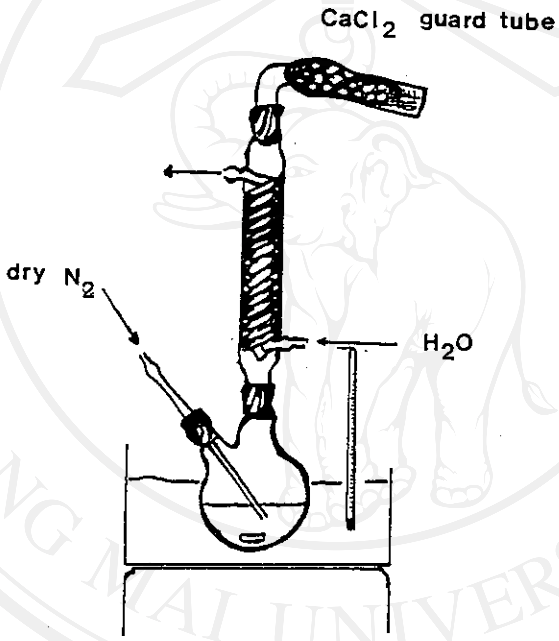

Fig. 3.3 : **Apparatus used for the purification of the crude product by hot ethanol extraction.**

In a typical purification, using the apparatus shown in Fig. 3.3, approximately 0.2 g of crude product was refluxed in 50 ml of absolute ethanol in the heating flask under a dry nitrogen atmosphere at 78-80 °C. Heating was continued for about 12 hours with constant stirring. The products obtained are described in Tables 3.2-3.5 in terms of their physical appearances and weights both before and after purification.

Table 3.2 : Block copolymerisation studies of glycolide and PEG 200 using aluminium triethyl as initiator: appearance of products before and after purification.

Monomer Ratio (mole %)	Polymerisation Temperature, °C					
	150		180		200	
G : PEG	crude	purified	crude	purified	crude	purified
100 : 0	white solid	-	pale yellow solid	-	pale yellow solid	-
0 : 100	X yellow liquid	-	X yellow liquid	-	X orange liquid	-
99 : 1	white solid	white solid	white solid with a slight yellow discoloration	pale yellow solid	yellow solid	pale yellow solid
97 : 3	white solid with a slight pale yellow discoloration	white solid	white solid with a slight yellow discoloration	pale yellow solid	brown solid with a slight yellow discoloration	pale brown solid
94 : 6	white solid with a slight pale yellow discoloration	white solid	white solid with a slight yellow discoloration	yellow solid	brown solid	pale brown solid
90 : 10	pale yellow solid	pale yellow solid	yellow viscous liquid	yellow solid	X brown viscous liquid	-

Key to Abbreviations and Symbols :

G = glycolide

PEG = poly(ethylene glycol)

X = polymerisation apparently did not occur or occurred to only a very limited extent; hence, purification was considered unnecessary

Table 3.3 : Block copolymerisation studies of glycolide and PEG 1500 using aluminium triethyl as initiator: appearance of products before and after purification.

Monomer Ratio (mole %)	Polymerisation Temperature, °C					
	150		180		200	
G : PEG	crude	purified	crude	purified	crude	purified
100 : 0	white solid	-	pale yellow solid	-	pale yellow solid	-
0 : 100	X yellow liquid	-	X orange liquid	-	X orange-red liquid	-
99 : 1	white solid	white solid	pale yellow solid	white solid	yellow solid	pale yellow solid
97 : 3	white solid with a slight yellow discoloration	white solid	white solid with a slight brown discoloration	white solid	yellow solid	pale brown solid
94 : 6	X brown viscous liquid	—	X brown viscous liquid	-	X dark brown viscous liquid	pale brown solid
90 : 10	X brown viscous liquid	-	X brown viscous liquid	-	X dark brown viscous liquid	-

Table 3.4 : Block copolymerisation studies of glycolide and PEG 200 using stannous oxalate as initiator: appearance of products before and after purification.

Monomer Ratio (mole %)	Polymerisation Temperature, °C					
	150		180		200	
G : PEG	crude	purified	crude	purified	crude	purified
100 : 0	white solid	-	white solid	-	white solid	-
0 : 100	X yellow viscous liquid	-	X pale brown viscous liquid	-	X brown viscous liquid	-
99 : 1	white solid	white solid	white solid	white solid	white solid with a slight brown discoloration	white solid
97 : 3	pale brown solid	white solid	pale brown solid with a slight yellow discoloration	white solid	brown solid	pale brown solid
94 : 6	white solid with a slight yellow discoloration	white solid	pale brown solid	white solid	brown solid	pale brown solid
90 : 10	brown solid	pale brown solid	X brown viscous liquid	-	X dark brown viscous liquid	-

Table 3.5 : Block copolymerisation studies of glycolide and PEG 1500 using stannous oxalate as initiator: appearance of products before and after purification.

Monomer Ratio (mole %)	Polymerisation Temperature, °C					
	150		180		200	
G : PEG	crude	purified	crude	purified	crude	purified
100 : 0	white solid	-	white solid	-	white solid	-
0 : 100	X yellow viscous liquid	-	X yellow viscous liquid	-	X yellow viscous liquid	-
99 : 1	white solid	white solid	brown solid	pale brown solid	brown solid	pale brown solid
97 : 3	pale brown solid	white solid	brown solid	pale brown solid	brown solid	pale brown solid
94 : 6	X yellow viscous liquid	-	X brown viscous liquid	-	X brown viscous liquid	-
90 : 10	X brown viscous liquid	-	X brown viscous liquid	-	X dark brown viscous liquid	-

The results of the copolymer extractions provide some qualitative indication as to whether or not the copolymers actually contain any copolymerised PEG. Following hot extraction in absolute ethanol, the resultant weight loss can be ascribed to the solubilization of such low molecular constituents as:

(1) unreacted glycolide
(2) unreacted PEG
(3) oligomeric products
(4) catalyst residues

Provided that the total weight loss on extraction did not exceed the initial weight of PEG in the comonomer feed, it can be concluded that the copolymer product must therefore contain at least some PEG, even though the exact amount remains unknown. The results are summarized in Tables 3.6-3.9.

Sample Calculation:

In Table 3.6, for the copolymerisation at 150 °C of :

G : PEG 200 = 99 : 1 mole %
= 5.000 : 0.087 g
theoretical 100 % copolymer yield = 5.087 g
weight of crude copolymer used in extraction = 2.030 g
theoretical weight of PEG in crude copolymer before extraction

$$= \frac{2.030 \times 0.087}{5.087} = 0.035 \text{ g}$$

actual weight loss from crude copolymer following extraction

$$= 0.025 \quad g$$

$$\text{i.e.,} < 0.035 \quad g$$

What this result serves to show is that the product is indeed a copolymer containing "bound" PEG, since all "free" PEG would have been removed by the extraction procedure.

Finally, in Table 3.6, for this sample:

$$\% \text{ weight loss} = \frac{0.025 \times 100}{2.030} = 1.23 \%$$

However, from these results alone, it is not possible to calculate the exact copolymer composition or to draw any firm conclusions as to the copolymer structure. This requires much more detailed study such as that provided by the DSC, TG and ^{1}H-NMR analyses described in later sections of this thesis.

Table 3.6 : Weight loss from poly(glycolic acid-b-oxyethylene) following purification: copolymer from PEG 200 using aluminium triethyl as initiator.

Monomer ratio G : PEG 200 (mole %)	Temperature of copolymerisation (°C)	Weight of PEG in crude copolymer before purification (g)	Weight loss after purification (g)	% Weight loss (%)
99 : 1	150	0.035	0.025	1.23
	180	0.033	0.025	1.26
	200	0.035	0.043	2.18
97 : 3	150	0.098	0.039	1.99
	180	0.109	0.059	2.94
	200	0.080	0.067	4.40
94 : 6	150	0.198	0.128	6.50
	180	0.216	0.193	9.53
	200	0.210	0.188	10.46
90 : 10	150	0.339	0.412	19.66
	180	0.331	0.361	19.56

Table 3.7 : Weight loss from poly(glycolic acid-b-oxyethylene) following purification: copolymer from PEG 1500 using aluminium triethyl as initiator.

Monomer ratio G : PEG 1500 (mole %)	Temperature of copolymerisation (°C)	Weight of PEG in crude copolymer before purification (g)	Weight loss after purification (g)	% Weight loss (%)
99 : 1	150	0.232	0.056	2.79
	180	0.233	0.079	3.91
	200	0.233	0.109	5.41
97 : 3	150	0.572	0.445	22.22
	180	0.579	0.438	21.61
	200	0.598	0.358	17.10

Table 3.8 : Weight loss from poly(glycolic acid-b-oxyethylene) following purification: copolymer from PEG 200 using stannous oxalate as initiator.

Monomer ratio G : PEG 200 (mole %)	Temperature of copolymerisation (°C)	Weight of PEG in crude copolymer before purification (g)	Weight loss after purification (g)	% Weight loss (%)
99 : 1	150	0.030	0.029	1.10
	180	0.029	0.021	1.22
	200	0.035	0.029	1.43
97 : 3	150	0.103	0.037	1.86
	180	0.101	0.062	3.10
	200	0.106	0.088	4.25
94 : 6	150	0.180	0.101	5.23
	180	0.188	0.105	5.57
	200	0.230	0.146	7.65
90 : 10	150	0.160	0.313	15.68
	180	0.322	0.425	21.25

Table 3.9 : Weight loss from poly(glycolic acid-b-oxyethylene) following purification: copolymer from PEG 1500 using stannous oxalate as initiator.

Monomer ratio G : PEG 1500 (mole %)	Temperature of copolymerisation (°C)	Weight of PEG in crude copolymer before purification (g)	Weight loss after purification (g)	% Weight loss (%)
99 : 1	150	0.216	0.203	0.092
	180	0.411	0.107	4.88
	200	0.218	0.211	10.83
97 : 3	150	0.575	0.414	20.56
	180	0.659	0.426	21.03
	200	0.738	0.628	31.07

From the results in Tables 3.6-3.9, some general conclusions can be drawn.

(1) In the majority of cases, the weight loss after purification (i.e., extraction + washing + vacuum oven drying to constant weight) was less than the theoretical amount of PEG contained in the crude sample. This supports the view that the products do contain at least some copolymerised PEG in their chemical structures.

(2) For a given monomer ratio, the % wight loss tends to increase with increasing temperature of copolymerisation. This may be due to (a) an increasing tendency for the glycolide monomer to homopolymerise with itself at higher temperatures, and/or (b) increasing thermal degradation of the copolymerised PEG blocks to extractable low molecular wight products. This latter suggestion (b) is supported by the observed increase in brown discoloration of the product with increasing temperature.

(3) As the mole % PEG in the comonomer feed increases from 1-10 %, the % wight loss on purification increases accordingly. This suggests that the weight loss may be partly due to unreacted PEG. However, more definitive evidence concerning this is provided by other techniques as will be described later.

(4) On comparing Tables 3.6 and 3.8, there do not appear to be any significant differences between using aluminium triethyl or stannous oxalate as initiator.

In this project, the copolymer products obtained were characterised by the following combination of analytical techniques:

(i) infrared spectroscopy (IR)
  - for structural characterisation
(ii) nuclear magnetic resonance spectroscopy (NMR)
  - for structural characterisation
(iii) differential scanning calorimetry (DSC)
  - for temperature transitions and crystallinity studies
(iv) thermogravimetry (TG)
  - for thermal stability studies
(v) dilute-solution viscometry
  - for molecular weight determination

3.3 Infrared Spectroscopy [21]

A Jasco Model IR-810 Infrared Spectrometer was used in this project. Figs. 3.4-3.5 show the infrared (IR) spectra of glycolic acid and glycolide. The spectra were obtained with the samples in the form of compressed KBr discs.

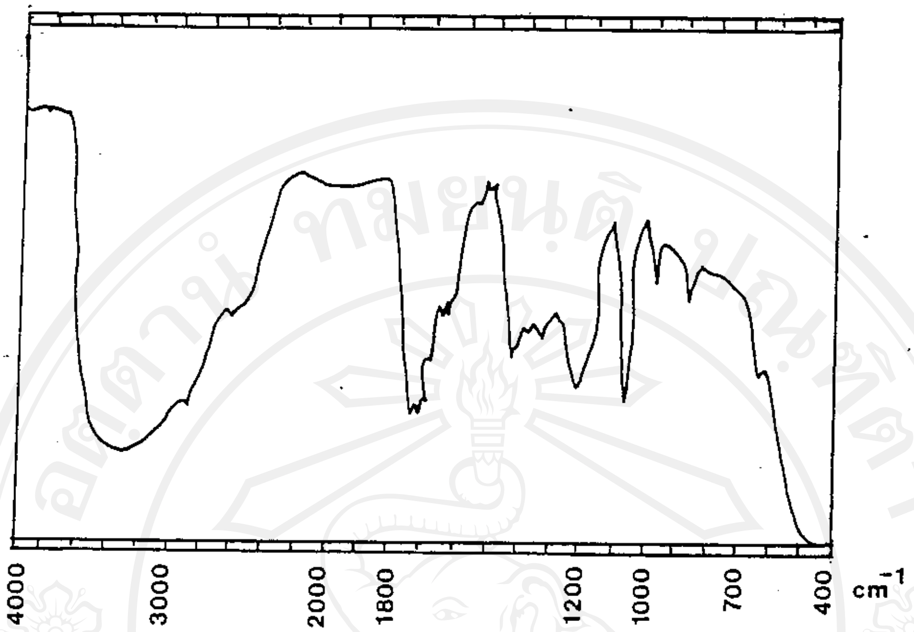

Fig. 3.4 : Infrared spectrum of glycolic acid.

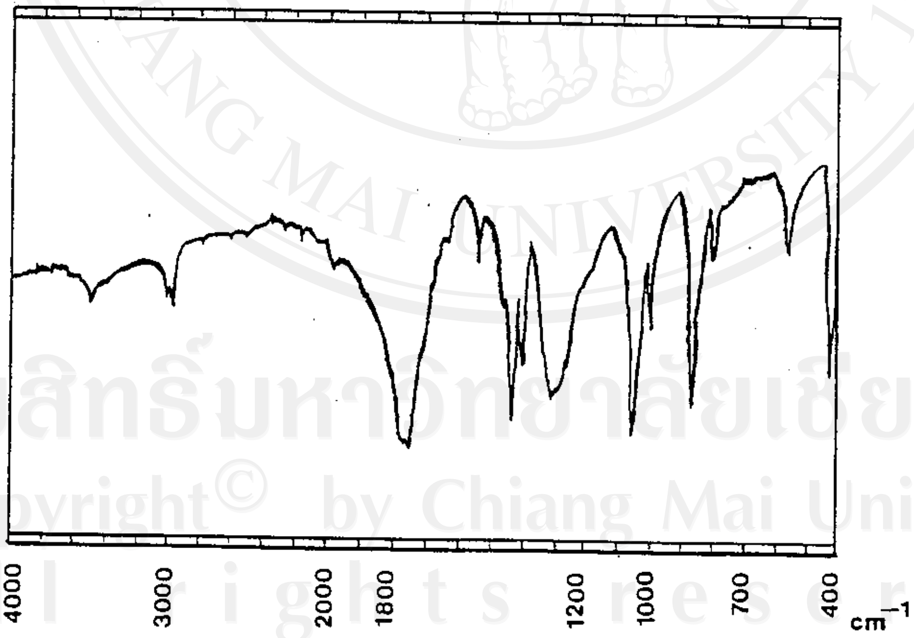

Fig. 3.5 : Infrared spectrum of glycolide.

The chemical structures of glycolic acid and glycolide are as follows:

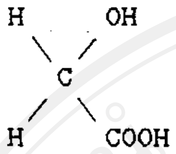

glycolic acid

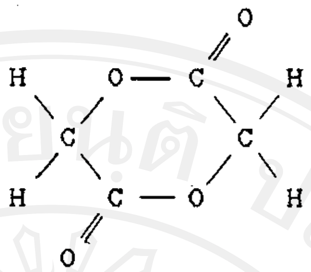

glycolide

The major bands in the spectra of glycolic acid and glycolide are compared in Table 3.10 and are consistent with the above structures. The transformation from the α-hydroxy acid to the cyclic diester is indicated in the spectra by the near-disappearance of the broad O-H band in glycolic acid and the shift to higher wavenumber of the C=O band in glycolide due to the effect of ring strain.

Table 3.10 : **Comparison of IR data of glycolic acid and glycolide.**

Vibrational Assignments	Wavenumber (cm^{-1})	
	Glycolic Acid	Glycolide
O-H str., in OH and COOH	≃ 3600-2500	(weak)
C-H str., in CH_2	≃ 3000	≃ 3000-2950
C=O str.	≃ 1760-1700	≃ 1780-1740
C-H bend, out-of-plane	1440-1350	1440, 1400
C-O str., acyl-O	≃ 1260-1200 $^{(a)}$	≃ 1320-1280 $^{(c)}$
alkyl-O	≃ 1100-1080 $^{(b)}$	1060 $^{(d)}$
O-H bend, in-plane	1440, 1350	
O-H bend, out-of-plane	≃ 1000-880	

KEY :

a = in $-\underline{\overset{\overset{O}{\|}}{C}-O}$ of glycolic acid

b = in $-\underline{\underset{|}{\overset{|}{C}}-O}$ of glycolic acid

c = in $-\underline{\overset{\overset{O}{\|}}{C}-O}$ of glycolide

d = in $-\underline{\underset{|}{\overset{|}{C}}-O}$ of glycolide

From the copolymerisations, it was expected that the copolymers would comprise adjoining poly(glycolic acid) and poly(ethylene glycol) blocks. In Figs. 3.6-3.9 are shown the infrared spectra of poly (glycolic acid), poly(ethylene glycol) PEG 200 and some of the copolymer products. The spectra were either obtained with the sample in the form of a KBr disc or, for PEG, using NaCl discs.

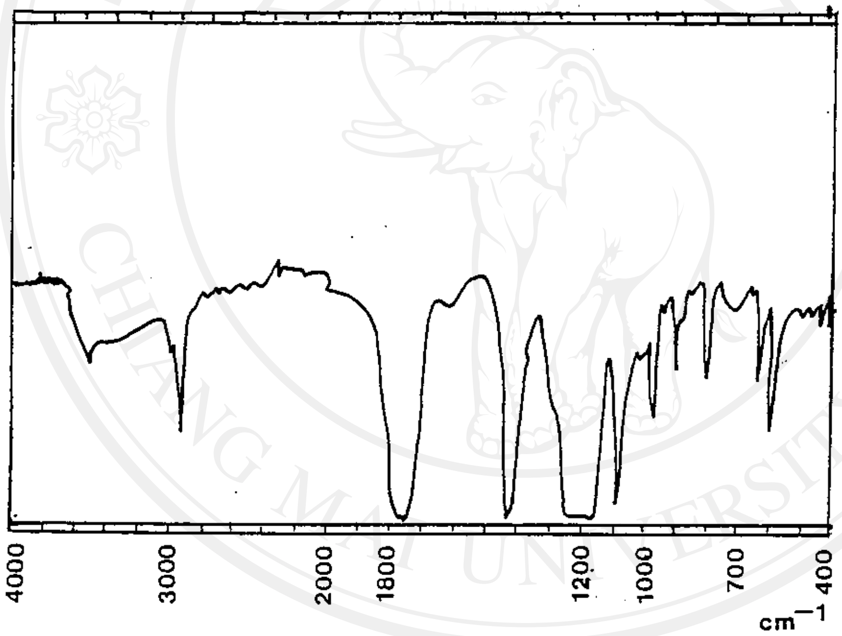

Fig. 3.6 : Infrared spectrum of poly(glycolic acid).

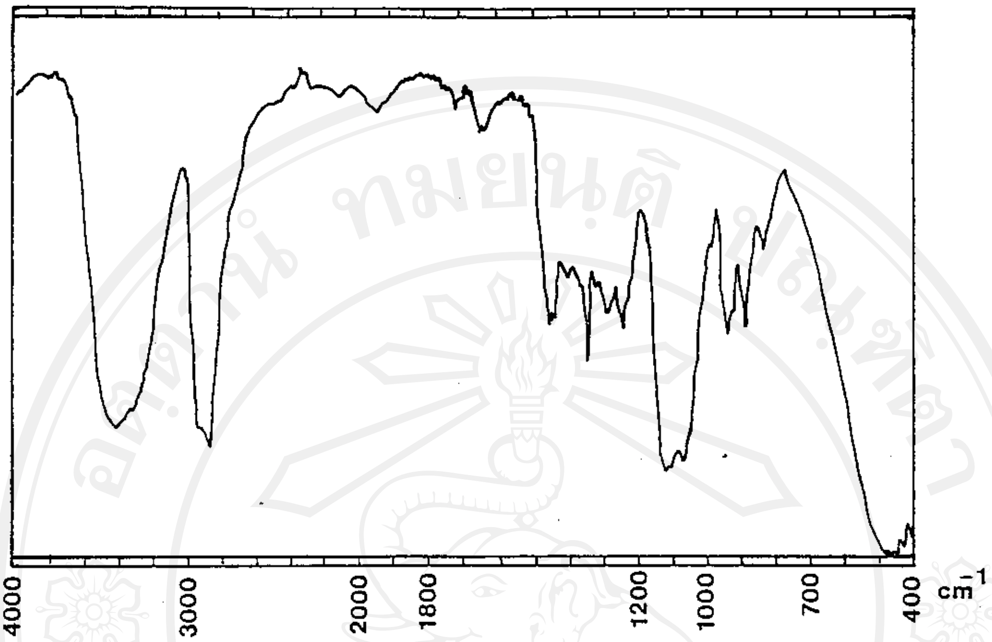

Fig. 3.7 : Infrared spectrum of poly(ethylene glycol)PEG 200.

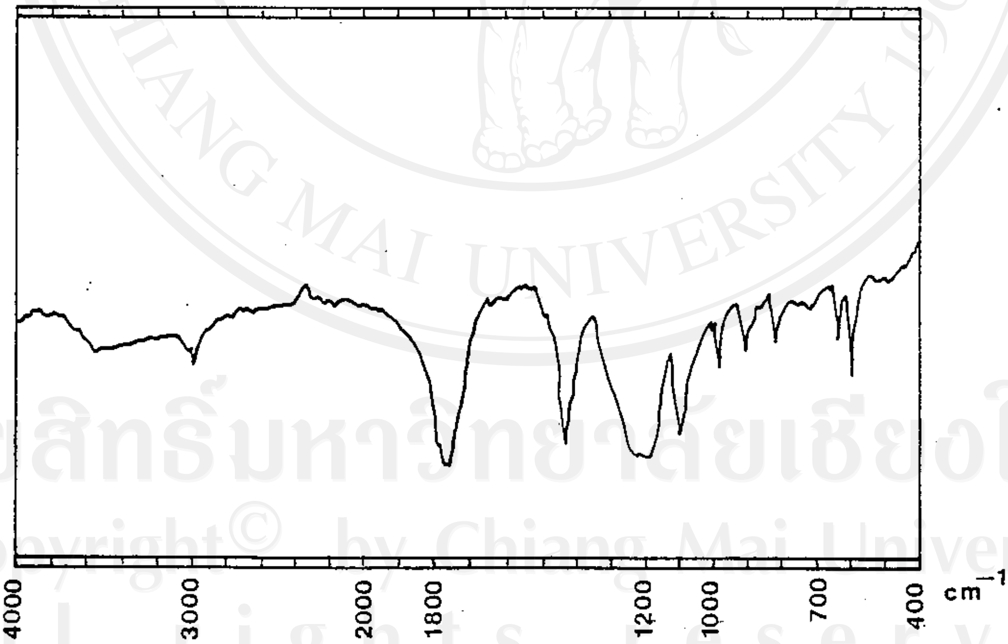

Fig. 3.8 : Infrared spectrum of poly(glycolic acid-b-oxyethylene)/
99:1/200°C/using aluminium triethyl as initiator.

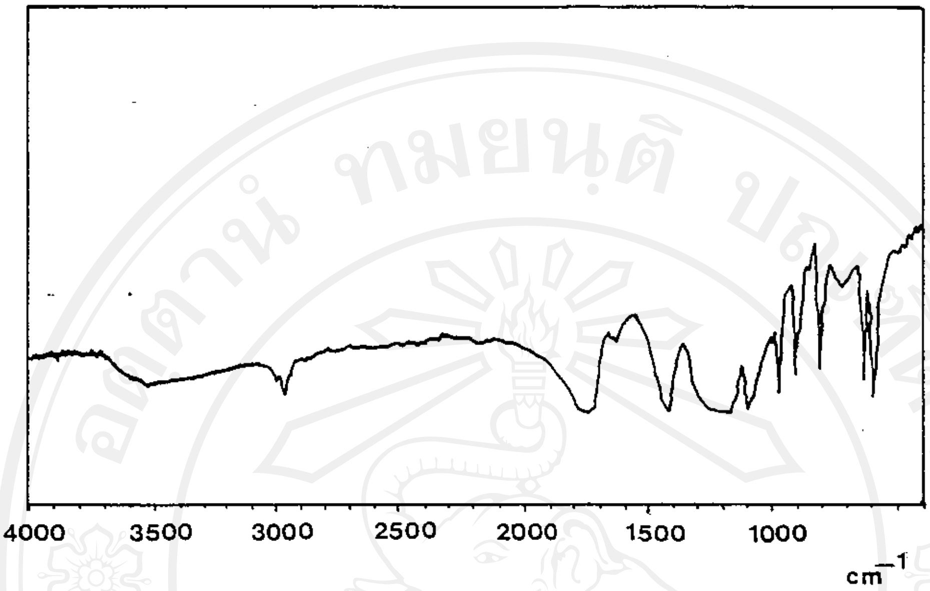

Fig. 3.9 : Infrared spectrum of poly(glycolic acid-b-oxyethylene)/ 97:3/200 °C/ using aluminium triethyl as initiator.

Table 3.11 : Comparison of IR data of poly(glycolic acid), poly(ethylene glycol), and poly(glycolic acid-b-oxyethylene).

Vibrational Assingments	Wavenumber (cm^{-1})		
	PGA	PEG 200	P(GA-b-PEG 200)
O-H str., in OH	≃ 3600-3400	≃ 3600-3200	≃ 3600-3400
O-H str., in COOH	(weak)	(strong)	(weak)
C-H str., in CH_2	≃ 3000-2980	≃ 2960-2850	≃ 3000-2980
C=O str.	≃ 1810-1720		≃ 1780-1740
C-H bend, out-of-plane	≃ 1440-1420	≃ 1450-1420	≃ 1440-1420
C-O str., in acyl-oxygen bonds	≃ 1260-1180		≃ 1260-1160
C-O str., in alkyl-oxygen bonds	≃ 1080	≃ 1140-1060	≃ 1120-1080
O-H bend, out-of-plane	≃ 980-800	≃ 940-840	≃ 980-820

The chemical structures of the two homopolymers and the block copolymer are compared below:

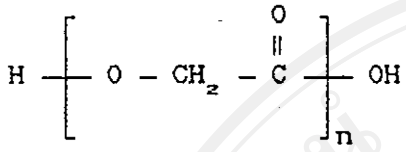

$$H-\left[O-CH_2-\overset{\overset{O}{\|}}{C}\right]_n-OH$$

poly(glycolic acid)

PGA

$$H-\left[O-CH_2-CH_2\right]_n-OH$$

poly(ethylene glycol)

PEG

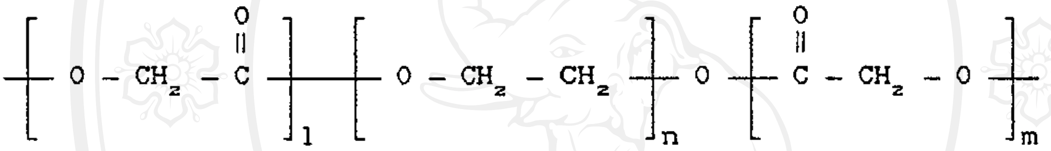

$$-\left[O-CH_2-\overset{\overset{O}{\|}}{C}\right]_l-\left[O-CH_2-CH_2\right]_n-O-\left[\overset{\overset{O}{\|}}{C}-CH_2-O\right]_m-$$

poly(glycolic acid-b-oxyethylene)

P(GA-b-PEG)

The major bands in their IR spectra are compared in Table 3.11. Not surprisingly, since PGA is by far the major component, the P(GA-b-PEG) copolymer spectra in Figs. 3.8-3.9 closely resemble that of the PGA homopolymer in Fig. 3.6. This is only to be expected if the copolymer chain is comprised of adjoining blocks as represented in the above structure.

Points to note in the copolymer spectra are:

(1) the absence of any strong O-H stretching band in the region 3600-3200 cm^{-1}; this indicates that the relatively short PEG blocks

are bonded through their OH end-groups to longer PGA blocks; hence, the weak O-H end-group bands in the copolymer spectra resemble that in the spectrum of PGA.

(2) the relatively sharp alkyl C-O stretching band in PGA alone at about 1080 cm^{-1} (Fig. 3.6) is seen to be broader (1120-1080 cm^{-1}) in the P(GA-b-PEG) copolymer spectra, presumably due to its overlap with the corresponding C-O band from the incorporated PEG segments.

3.4 Proton Nuclear Magnetic Resonance (^{1}H-NMR) Spectroscopy [22]

A Bruker Model AFC-200 MHz Nuclear Magnetic Resonance Spectrometer was used in this project. The ^{1}H-NMR spectra of PGA, PEG and P(GA-b-PEG 200) are shown in Figs. 3.10-3.14. The relative are as under the various resonance peaks, as calculated from the integration lines, are directly proportional to the relative numbers of protons to which they correspond. This enables the copolymer composition to be determined. The chemical shifts and corresponding proton assignments are tabulated in Tables 3.12-3.16.

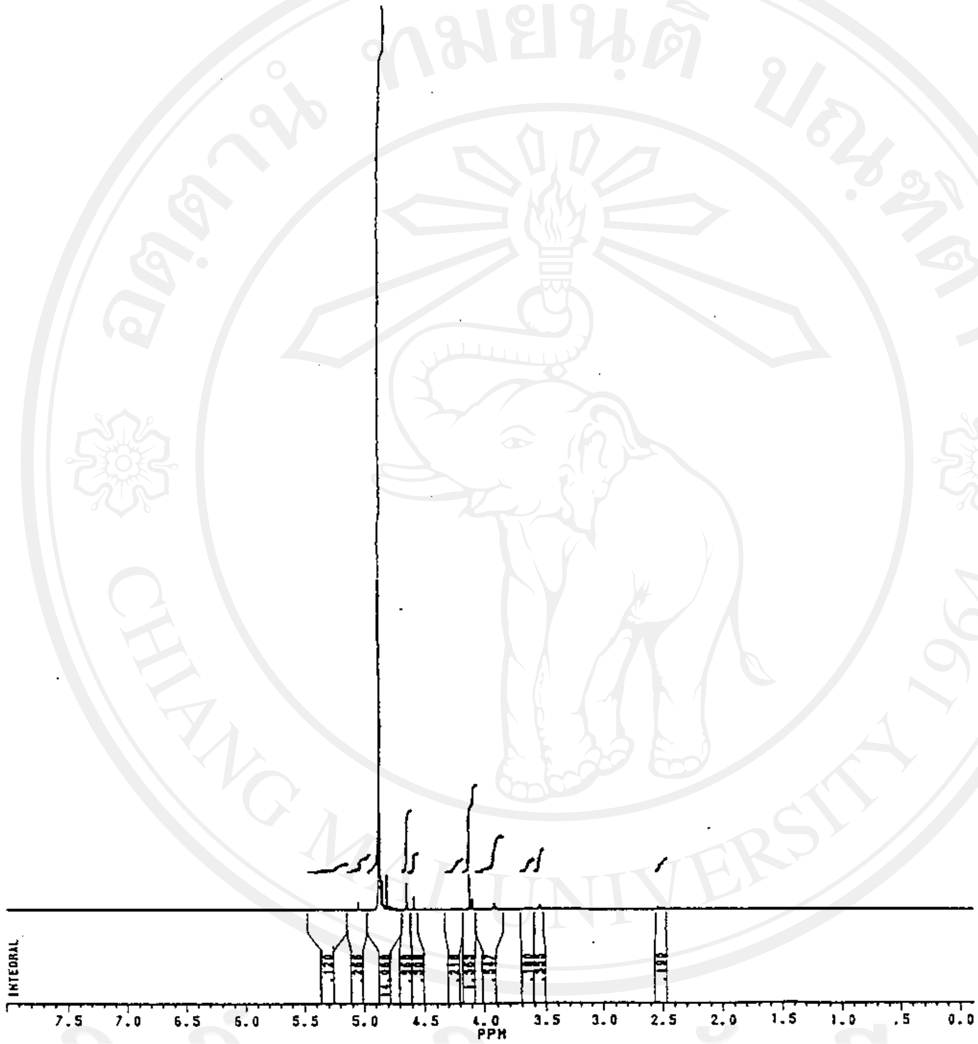

Fig. 3.10 : 200 MH$_z$ ^{1}H-NMR spectrum of PGA synthesized at 200 °C using aluminium triethyl as initator; solvent = d$_6$-DMSO at 90 °C.

Table 3.12 : **Interpretation of ^{1}H-NMR spectrum of PGA synthesized at 200 °C using aluminium triethyl as initiator, as shown in Fig. 3.10.**

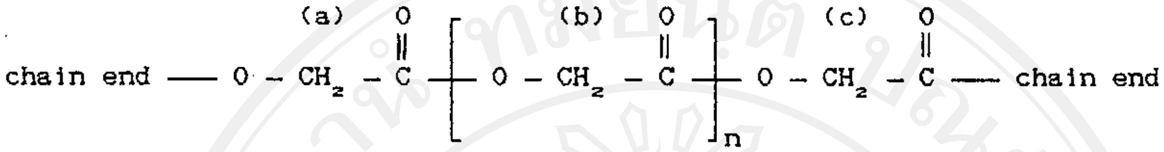

$$\text{chain end} - O - \overset{(a)}{CH_2} - \overset{O}{\overset{\|}{C}} - \left[O - \overset{(b)}{CH_2} - \overset{O}{\overset{\|}{C}} \right]_n - O - \overset{(c)}{CH_2} - \overset{O}{\overset{\|}{C}} - \text{chain end}$$

Proton Assignment	Chemical Shift (δ)
a	4.13, 4.09
b	4.88 4.85, 4.81
c	4.65, 4.58
unassigned peak *	3.93
d_6-DMSO solvent	2.54

* possibly due to H_2O impurity in solvent
DMSO is known to be hygroscopic

NOTE: other small peaks not listed in the table could be due to protons in $Al(C_2H_5)_3$ initiator residues at the chain ends

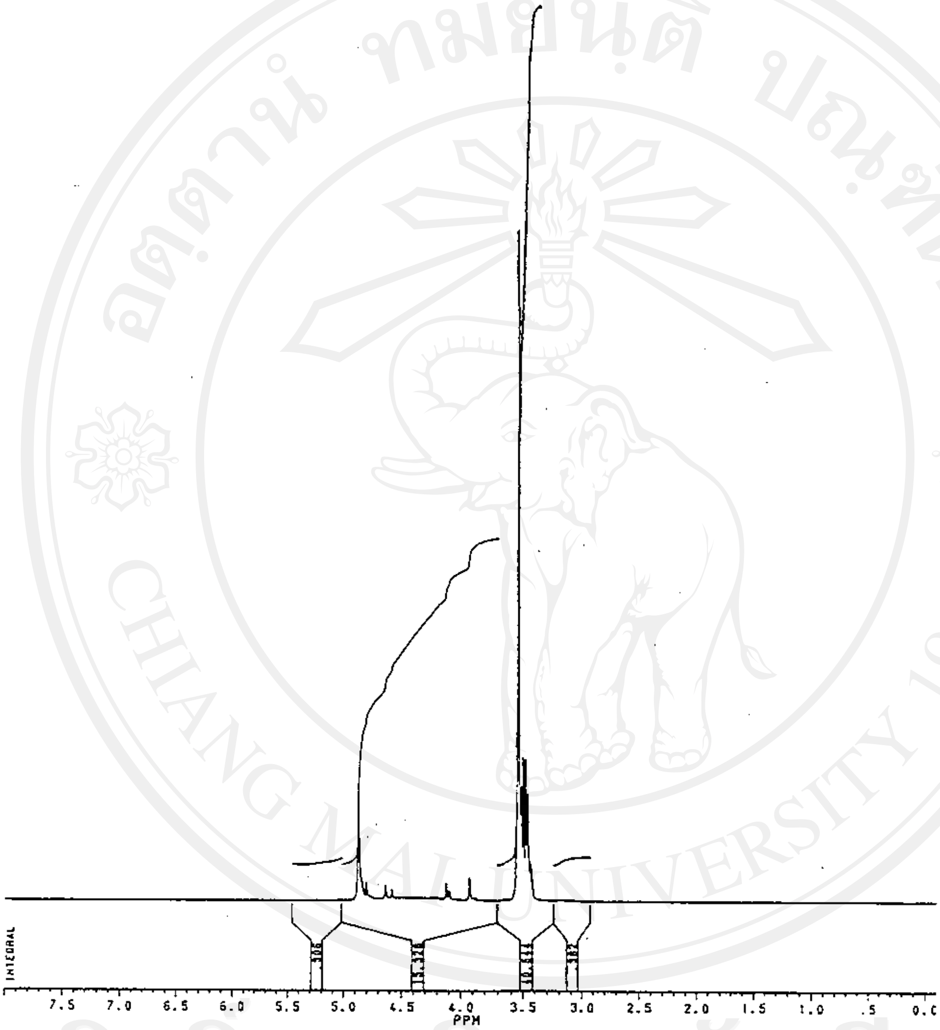

Fig. 3.11 : 200 MHz ^{1}H-NMR spectrum of PEG 200 in d_6-DMSO at 90 °C.

Table 3.13 : Interpreatation of ^{1}H-NMR spectrum of PEG 200, as shown in Fig. 3.11.

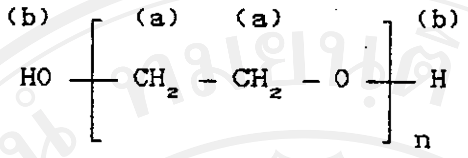

$$\overset{(b)}{HO}-\left[\overset{(a)}{CH_2}-\overset{(a)}{CH_2}-O\right]_n-\overset{(b)}{H} \qquad \text{for PEG 200} \quad n \simeq 4-5$$

Proton Assignment	Chemical Shift (δ)
a	3.55, 3.50
b	4.87
unassigned peak *	3.43

* possibly due to H_2O impurity in DMSO solvent

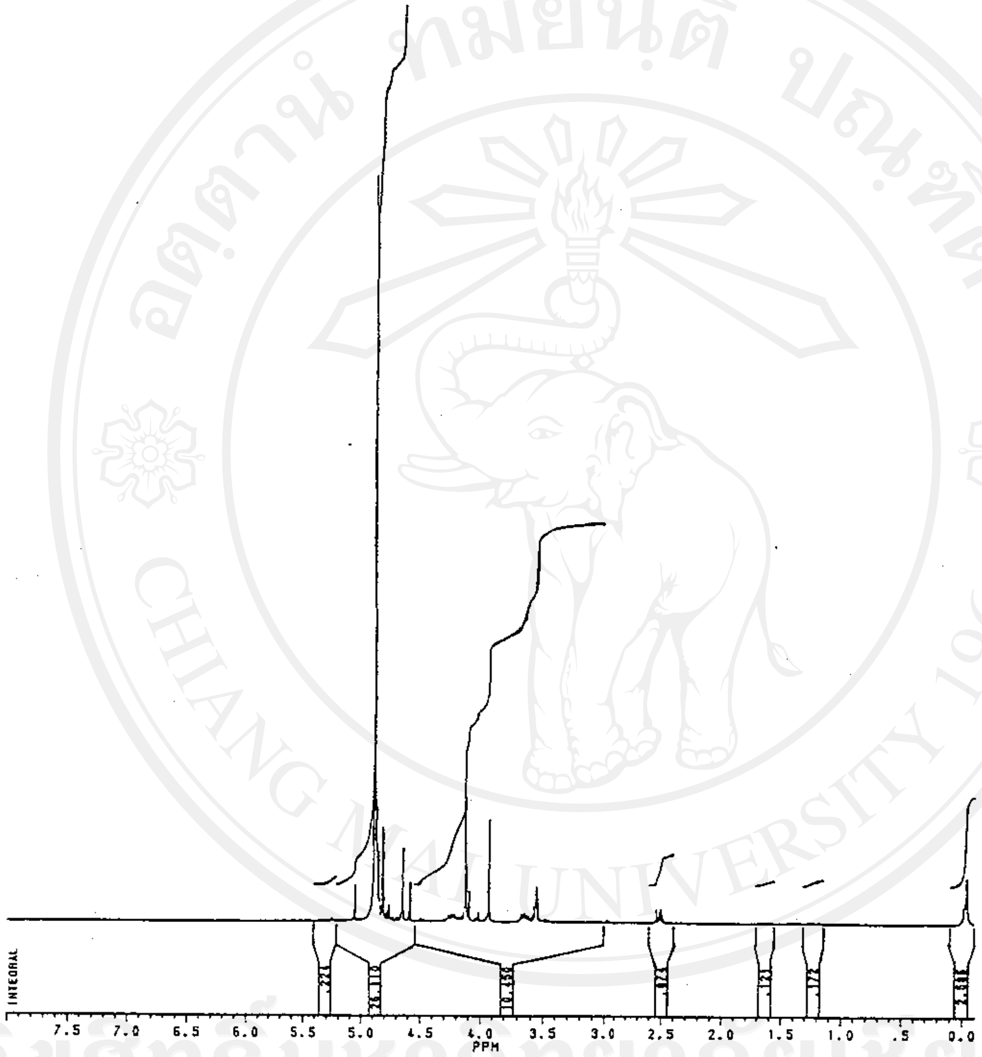

Fig. 3.12 : 200 MHz ^{1}H-NMR spectrum of P(GA-b-PEG 200) 99:1 synthesized at 200 °C using aluminium triethyl as initiator; solvent = d_6-DMSO at 90 °C.

Table 3.14 : Interpretation of ^{1}H-NMR spectrum of P(GA-b-PEG 200) 99:1 synthesized at 200 °C using aluminium triethyl as initator, as shown in Fig. 3.12.

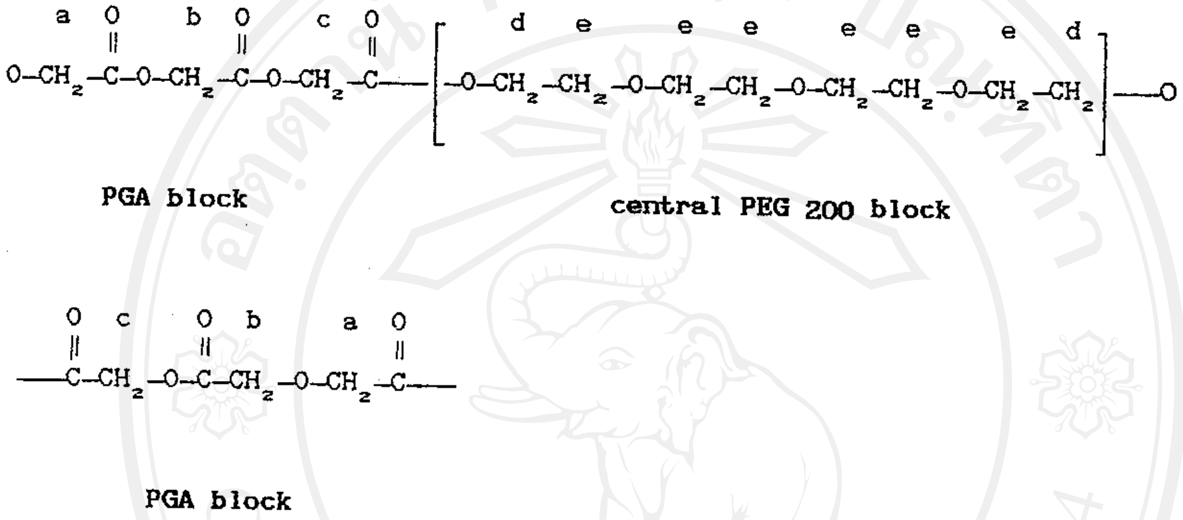

Proton Assignment	Chemical Shift (δ)
a	4.13, 4.10
b	4.88
	4.87, 4.81
c	4.65
d	4.09
e	3.55
unassigned peak	3.93
d_6-DMSO solvent	2.51

From the peak area integrations of the assigned methylene (a, b, c, d, e) peaks in Fig. 3.12, the copolymer composition is determined as follows:

$$\underset{\text{glycolic units}}{OCH_2CO} \quad : \quad \underset{\text{oxyethylene units}}{OCH_2CH_2}$$

$$\frac{\text{total area of glycolic unit peaks}}{2} : \frac{\text{total area of oxyethylene unit peaks}}{4}$$

$$115 : 4$$

$$29 : 1$$

$$\begin{aligned}\text{Copolymer Composition} &= OCH_2CO : OCH_2CH_2 \\ &= 29 : 1 \quad \text{(by mole)}\end{aligned}$$

Converting this repeat unit ratio into a comonomer ratio:

$$\begin{aligned}\text{Copolymer Composition} &= \frac{\text{moles of glycolide}}{\text{moles of PEG 200}} \\ &= \frac{\text{moles of glycolic units/2}}{\text{moles of oxyethylene units/4.55}} \\ &= \frac{29/2}{1/4.55}\end{aligned}$$

(where 4.55 = average value of n in PEG 200)

$$= \frac{14.5}{0.22}$$

$$= 65.25$$

$$\simeq 65$$

This comonomer mole ratio of 65 : 1 (98.5 : 1.5) in the final copolymer composition corresponds closely to the 99 : 1 mole % ratio of the initial comonomer feed.

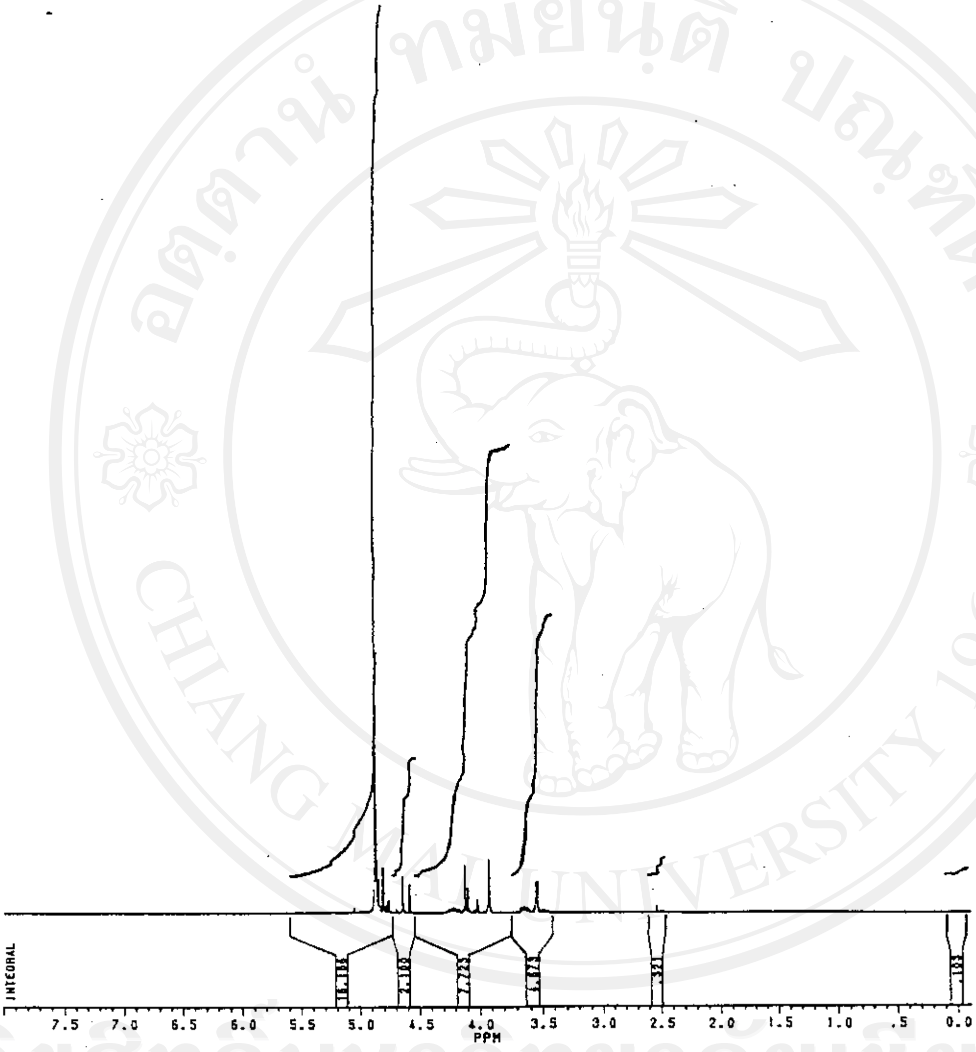

Fig. 3.13 : 200 MHz ^{1}H-NMR spectrum of P(GA-b-PEG 200) 97:3 synthesized at 200 °C using aluminium triethyl as initiator; solvent = d_6-DMSO at 90 °C.

<u>Table 3.15</u> : **Interpretation of ^{1}H-NMR spectrum of P(GA-b-PEG 200) 97:3 synthesized at 200 °C using aluminium triethyl as initiator, as shown in Fig. 3.13.**

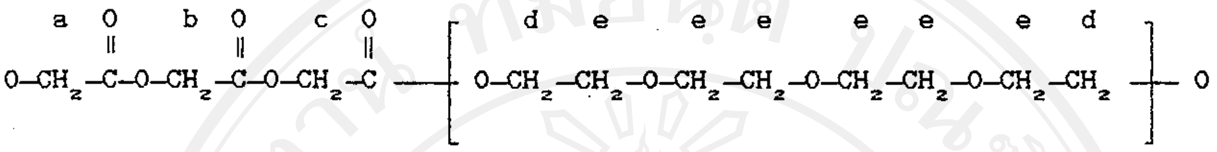

$$\overset{a}{\mathrm{O{-}CH_2}}{-}\overset{\overset{\mathrm{O}}{\|}}{\mathrm{C}}{-}\overset{b}{\mathrm{O{-}CH_2}}{-}\overset{\overset{\mathrm{O}}{\|}}{\mathrm{C}}{-}\overset{c}{\mathrm{O{-}CH_2}}{-}\overset{\overset{\mathrm{O}}{\|}}{\mathrm{C}}{-}\left[\mathrm{O{-}}\overset{d}{\mathrm{CH_2}}{-}\overset{e}{\mathrm{CH_2}}{-}\mathrm{O{-}}\overset{e}{\mathrm{CH_2}}{-}\overset{e}{\mathrm{CH_2}}{-}\mathrm{O{-}}\overset{e}{\mathrm{CH_2}}{-}\overset{e}{\mathrm{CH_2}}{-}\mathrm{O{-}}\overset{e}{\mathrm{CH_2}}{-}\overset{d}{\mathrm{CH_2}}\right]{-}\mathrm{O}$$

PGA block **central PEG 200 block**

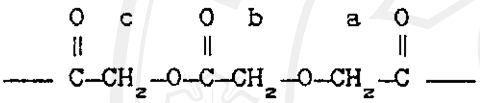

$$-\overset{\overset{\mathrm{O}}{\|}}{\mathrm{C}}{-}\overset{c}{\mathrm{CH_2}}{-}\mathrm{O}{-}\overset{\overset{\mathrm{O}}{\|}}{\mathrm{C}}{-}\overset{b}{\mathrm{CH_2}}{-}\mathrm{O}{-}\overset{a}{\mathrm{CH_2}}{-}\overset{\overset{\mathrm{O}}{\|}}{\mathrm{C}}-$$

PGA block

Proton Assignment	Chemical Shift (δ)
a	4.13
b	4.87
	4.85, 4.84, 4.81
c	4.65
d	4.09
e	3.55
unassigned peak	3.93, 0.05
d_6-DMSO solvent	2.50

From the peak area integrations of the various methylene (a, b, c, d, e) peaks in Fig. 3.13, the copolymer composition is again determined as:

OCH_2CO	:	OCH_2CH_2
glycolic units	:	oxyethylene units
14	:	1

Copolymer Composition : OCH_2CO : OCH_2CH_2

= 14 : 1 (by mole)

Via a similar calculation to that just described, this OCH_2CO: OCH_2CH_2 unit ratio converts to a comonomer mole ratio in the copolymer of:

glycolide : PEG 200 = 31.8 : 1 (by mole)

= 97.0 : 3.0 (mole %)

This corresponds exactly to the 97:3 mole % ratio of the initial comonomer feed.

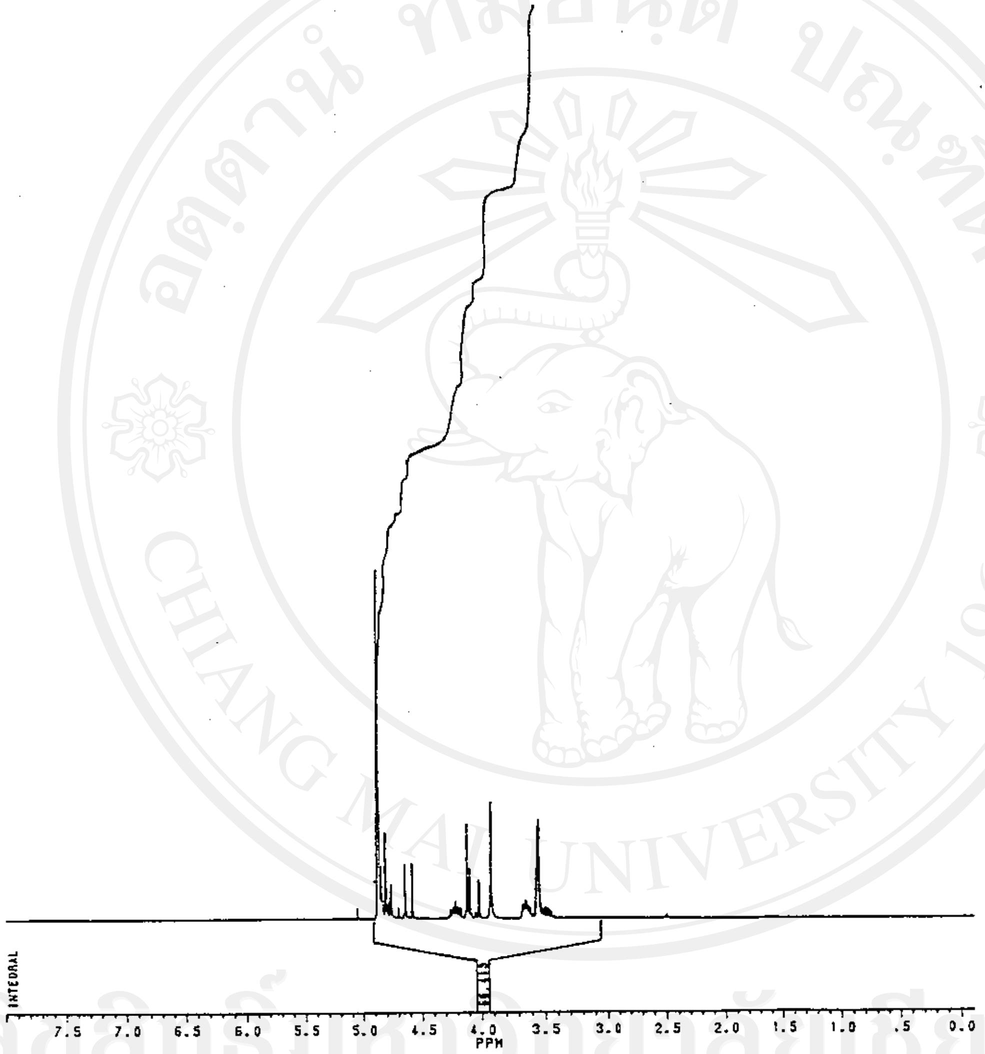

Fig. 3.14 : 200 MHz ^{1}H-NMR spectrum of P(GA-b-PEG 200) 94:6 synthesized at 200 °C using aluminium triethyl as initiator, solvent d_6-DMSO at 90 °C.

<u>Table 3.16</u> : Interpretation of the ^{1}H-NMR spectrum of P(GA-b-PEG 200) 94:6 synthesized at 200 °C using aluminium triethyl as initiator, as shown in Fig. 3.14.

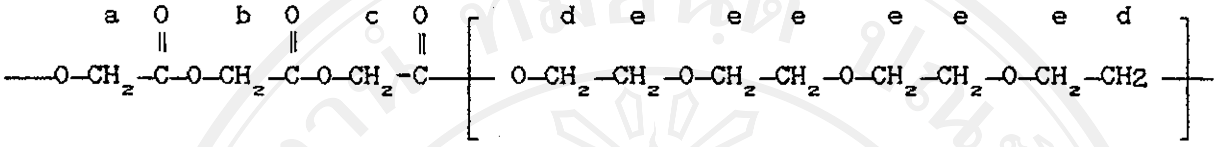

$$-O-\overset{a}{CH_2}-\overset{\overset{O}{\|}}{C}-O-\overset{b}{CH_2}-\overset{\overset{O}{\|}}{C}-O-\overset{c}{CH_2}-\overset{\overset{O}{\|}}{C}-\left[\,O-\overset{d}{CH_2}-\overset{e}{CH_2}-O-\overset{e}{CH_2}-\overset{e}{CH_2}-O-\overset{e}{CH_2}-\overset{e}{CH_2}-O-\overset{e}{CH_2}-\overset{d}{CH2}\,\right]-$$

PGA block **central PEG 200 block**

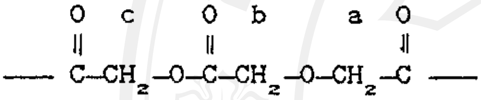

$$-\overset{\overset{O}{\|}}{C}-\overset{c}{CH_2}-O-\overset{\overset{O}{\|}}{C}-\overset{b}{CH_2}-O-\overset{a}{CH_2}-\overset{\overset{O}{\|}}{C}-$$

PGA block

Proton Assignment	Chemical Shift (δ)
a	4.13
b	4.88
	4.87, 4.85, 4.81
c	4.65
d	4.09
e	3.55
$-CH_2OCH_2-$ (DEG)	3.50
unassigned peak	3.93
d_6-DMSO solvent	2.50

From the peak area integrations of the methylene (a, b, c, d, e) peaks in Fig. 3.14, the copolymer composition is determined as:

OCH_2CO : OCH_2CH_2
glycolic units : oxyethylene units
9 : 1 (by mole)

which, in turn, corresponds to a comonomer mole ratio of

$$\begin{aligned}
\text{Copolymer Composition} &= \text{glycolide} : \text{PEG 200} \\
&= \frac{9}{2} : \frac{1}{4.55} \\
&= 4.5 : 0.22 \\
&= 20.5 : 1 \quad \text{(by mole)} \\
&= 95.3 : 4.7 \quad \text{(mole \%)}
\end{aligned}$$

This result again agrees closely with the initial comonomer feed mole % ratio of 94:6.

Table 3.17 : **Comparison of the comonomer mole % ratios in the initial comonomer feeds and in the resulting copolymer compositions for the P(GA-b-PEG 200) / $Al(C_2H_5)_3$ / 200 °C samples.**

Initial Comonomer Feed Glycolide : PEG 200 (mole %)	Copolymer Composition Glycolide : PEG 200 (mole %)
99 : 1	98.5 : 1.5
97 : 3	97.0 : 3.0
94 : 6	95.3 : 4.7

In this project, the copolymer products obtained have been characterised by a range of analytical techniques: IR, ^{1}H-NMR and, still to follow, DSC, TG and dilute-solution viscometry. However, only ^{1}H-NMR provides direct quantitative evidence confirming that the copolymers do actually contain copolymerised PEG in their chemical structures. The other techniques, while supporting this NMR view, provide only indirect evidence of PEG inclusion.

From the results in Table 3.17, the comonomer mole % ratios in the copolymer compositions correspond very closely with those of the initial comonomer feeds. From this, it can be concluded that, under the conditions of synthesis employed in this project, the PEG 200 has been successfully incorporated into the block copolymer structure in almost quantitative fashion. However, the precise microstructure (i.e., number of blocks per chain, average PGA block length, etc.) remains unknown. Elucidation of this copolymer microstructure should form the subject of a future research project.

3.5 Determination of Melting Point/Range

3.5.1 Visual Observation

A Buchi SMP-20 Melting Point Determinator was used to determine the melting range (T_m) of poly(glycolic acid-b-oxyethylene) by visual observation. The results are shown in Table 3.21-3.24.

3.5.2 Differential Scanning Calorimetry (DSC)

3.5.2.1 Theory and Instrumentation [23, 24]

Differential scanning calorimetry (DSC) is a technique of non-equilibrium calorimetry in which the heat flow into or from a sample and reference is measured as some function of time or temperature. It can show how strongly polymer properties are influenced by their thermal treatment. The most frequent application of DSC has been to the measurement of transition heats and temperatures.

For precise measurement of heats of transition, it is necessary to ensure:

(a) precise sample weighing;

(b) precise measurement of the peak area lying under the endotherm or exotherm caused by the transition.

The area of the transition peak is directly proportional to the energy of the change per unit weight (heat of fusion, ΔH_f, in terms of J/g). DSC is also widely used to determine the percent crystallinity of a polymer via heats of fusion [25].

In this project, the particular instrument used was a Perkin-Elmer DSC7 Differential Scanning Calorimeter which was a state-of-the-art, computer-controlled laboratory instrument. The theory of operation of the DSC7 is based on the power compensated "null-balance" DSC principle in which energy absorbed or evolved by the sample is compensated by adding or subtracting an equivalent amount of electrical energy to a heater located in the sample holder. The Perkin-Elmer DSC design measures the energy of a transition directly and thus provides true calorimetric information.

3.5.2.2 Analytical Procedure

The following operating conditions were employed for each sample analysis:

Parameters:

Final Temp : 250.00 °C
Start Temp : 25.00 °C
Scanning Rate : 10.00 °C/min
Y Range : 40.00 mW
Sample Weight : approx. 5 mg

Baseline Status : Y
Multitasking : Y or N (optional)

Conditions:

End Condition : S
Load Temp : 25.00 °C
Go To Temp Rate : 50.00 °C
Event 1 Time : 0.00 min.
Event 2 Time : 0.00 min.
Data Delay : 0.00 min.
Time at T Start : 0.00 min.
Time at T Final : 0.00 min.
Y Initial Value : 10.00 mW

In addition, a N_2 purge gas pressure of 20 lbs/in^2 (flow-rate = approx. 40 ml.min) was employed throughout, as recommended by the instrument manufacturer. The N_2 gas was high-purity (99.9 %), oxygen-free grade and was further pre-dried by passage through an in-line drying column containing both calcium sulphate ('Drierite') and molecular sieves (type 4 Å) as desiccants.

3.5.2.3 Results

The DSC thermograms in Figs. 3.15-3.21 and the data in Tables 3.18-3.20 compare the melting characteristics of both the crude and purified copolymers synthesized under various conditions.

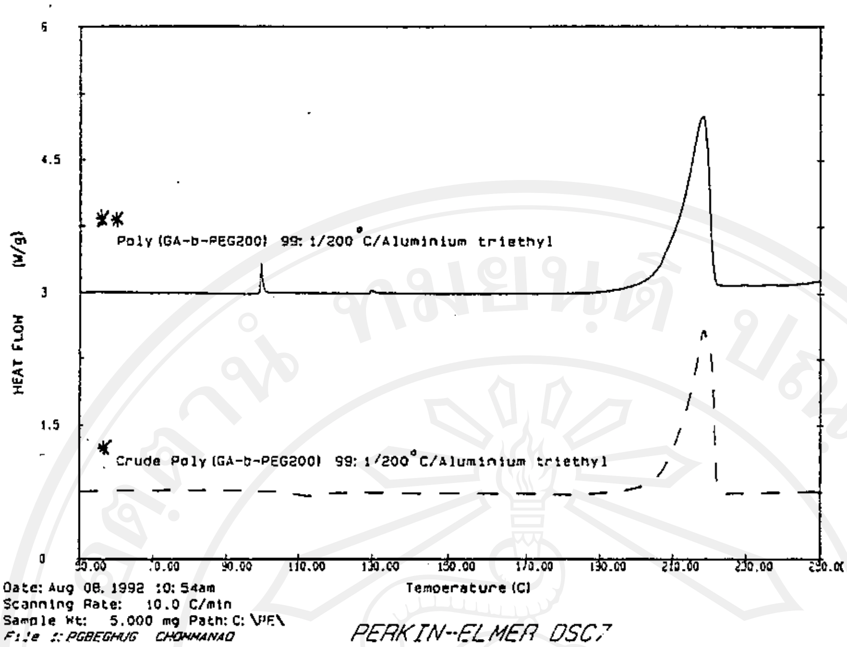

Fig. 3.15 : Comparison of the DSC thermograms of crude and purified copolymers

* Crude P(GA-b-PEG 200)99:1/200 °C/aluminium triethyl

** Purified P(GA-b-PEG 200)99:1/200 °C/aluminium triethyl

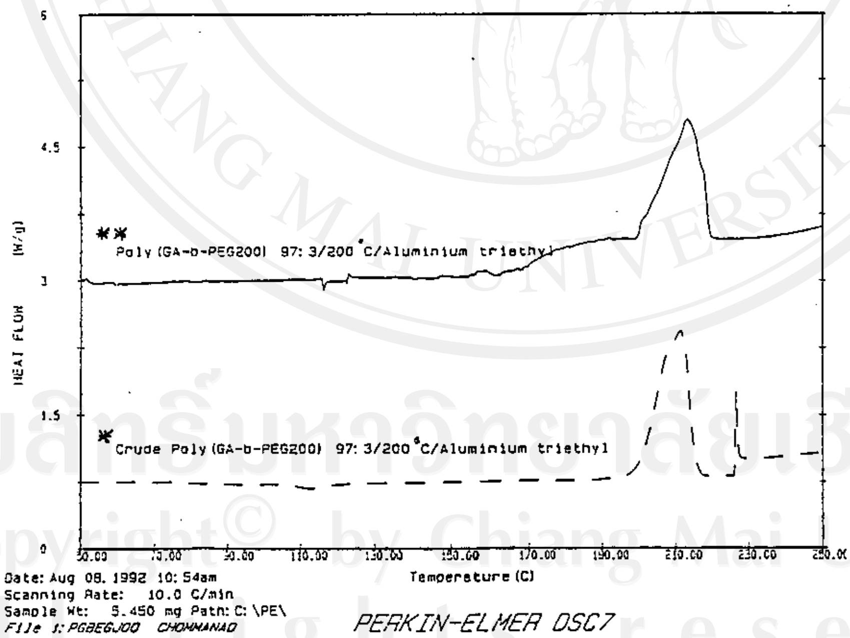

Fig. 3.16 : Comparison of the DSC thermograms of crude and purified copolymers

* Crude P(GA-b-PEG 200) 97:3/200 °C/aluminium triethyl

** Purified P(GA-b-PEG 200) 97:3/200 °C/aluminium triethyl

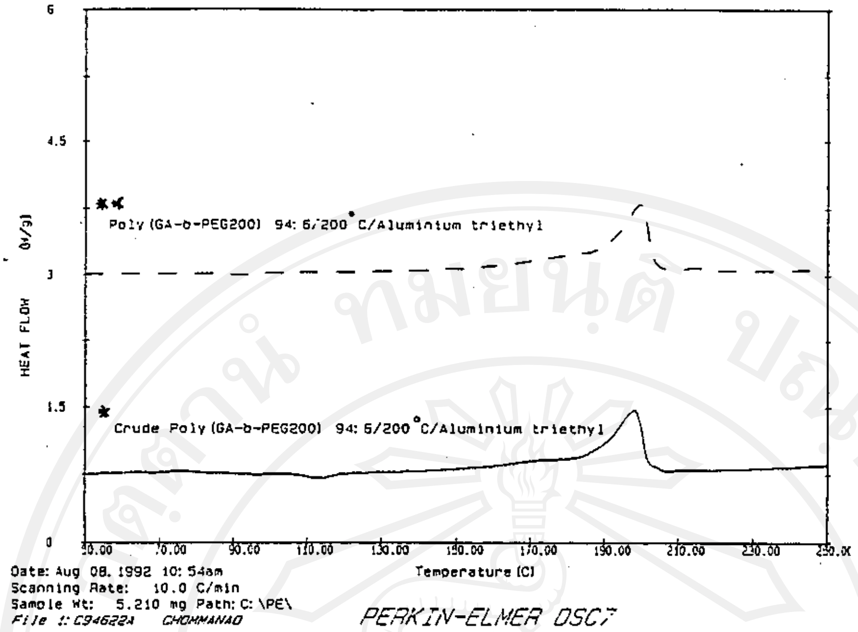

Fig. 3.17 : Comparison of the DSC thermogrames of crude and purified copolymers

* Crude P(GA-b-PEG 200) 94:6/200°C/aluminium triethyl

** Purified P(GA-b-PEG 200) 94:6/200°C/aluminium triethyl

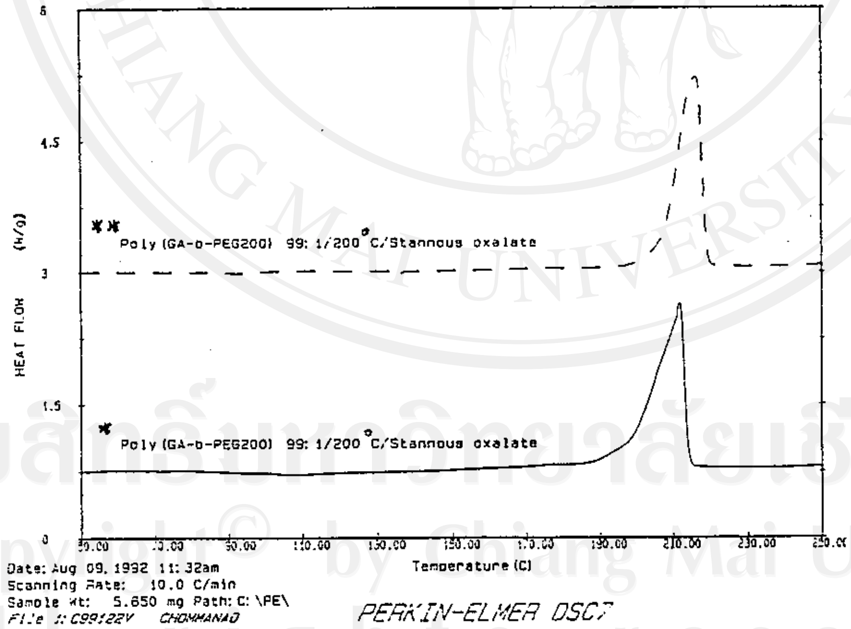

Fig. 3.18 : Comparison of the DSC thermogrames of crude and purified copolymers

* Crude P(GA-b-PEG 200) 99:1/200°C/stannous oxalate

** Purified P(GA-b-PEG 200) 99:1/200°C/stannous oxalate

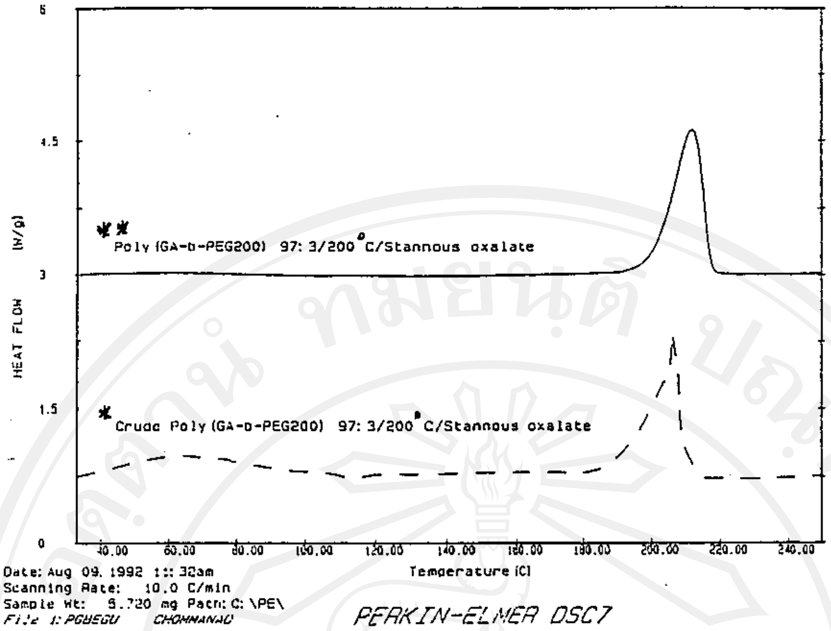

Fig. 3.19 : Comparison of the DSC thermogrames of crude and purified copolymers

* Crude P(GA-b-PEG 200) 97:3/200 °C/stannous oxalate

** Purified P(GA-b-PEG 200) 97:3/200 °C/stannous oxalate

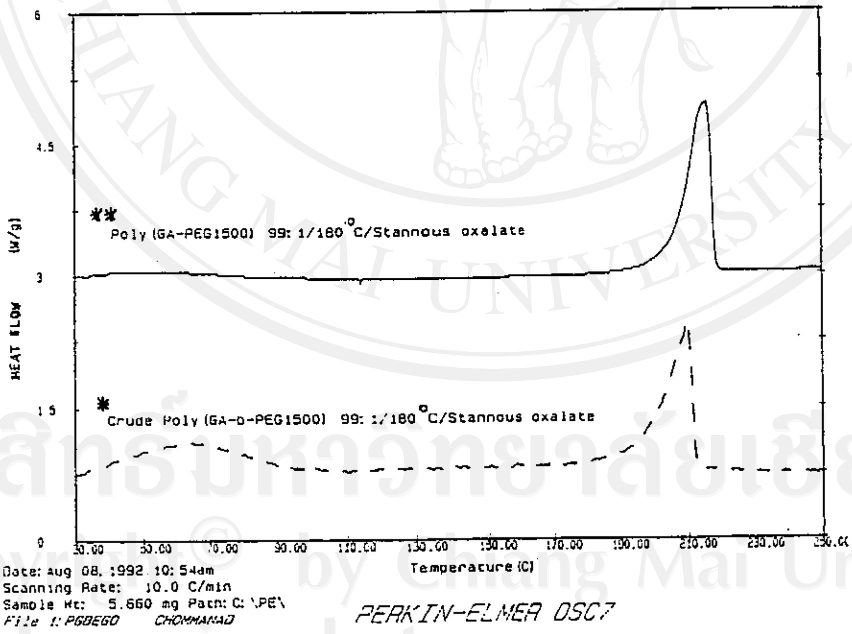

Fig. 3.20 : Comparison of the DSC thermograms of crude and purified copolymers

* Crude P(GA-b-PEG 1500) 99:1/180 °C/stannous oxalate

** Purified P(GA-b-PEG 1500) 99:1/180 °C/stannous oxalate

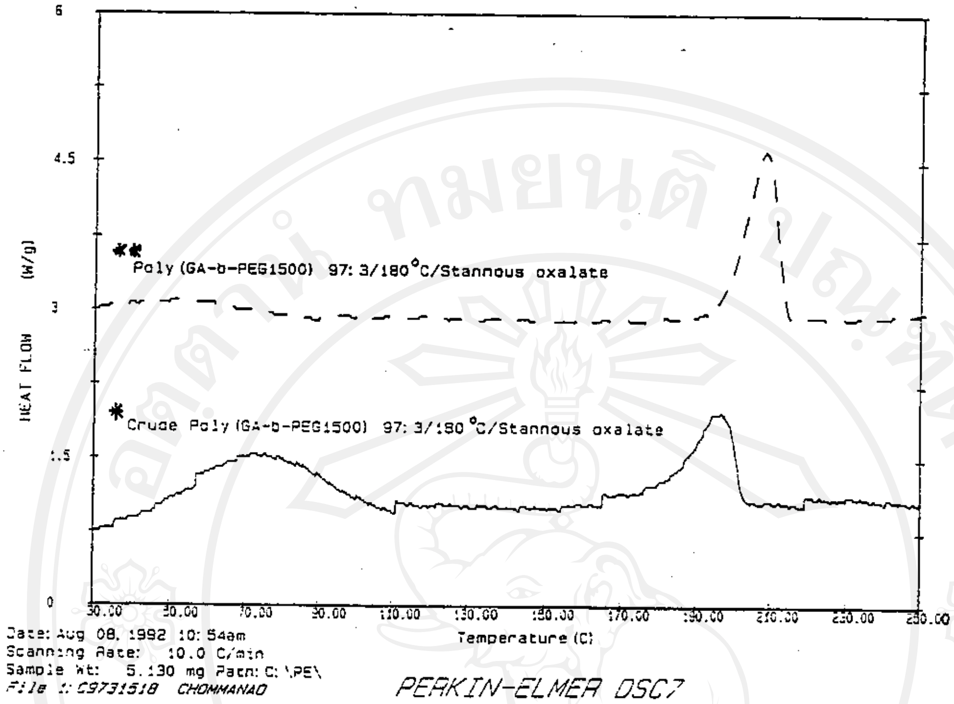

Fig. 3.21 : Comparison of the DSC thermograms of crude and purified copolymers

* Crude P(GA-b-PEG 1500) 97:3/180 °C/stannous oxalate

** Purified P(GA-b-PEG 1500) 97:3/180 °C/stannous oxalate

Table 3.18 : Comparison of DSC melting points (peak T_m) of crude and purified P(GA-b-PEG 200): aluminium triethyl as initator.

Monomer Ratio (mole %) G : PEG	Polymerisation Temperature (°C)	Peak T_m	
		Crude (°C)	Purified (°C)
99 : 1	200	218.23	218.08
97 : 3	200	211.27	213.32
94 : 6	200	198.17	199.64

Table 3.19 : Comparison of DSC melting points (peak T_m) of crude and purified P(GA-b-PEG 200): stannous oxalate as initiator.

Monomer Ratio (mole %) G : PEG	Polymerisation Temperature (°C)	Peak T_m	
		Crude (°C)	Purified (°C)
99 : 1	200	211.76	216.17
97 : 3	200	205.83	211.73

Table 3.20 : Comparison of DSC melting points (peak T_m) of crude and purified P(GA-b-PEG 1500): stannous oxalate as initiator.

Monomer Ratio (mole %) G : PEG	Polymerisation Temperature (°C)	Peak T_m	
		Crude (°C)	Purified (°C)
99 : 1	180	209.52	215.60
97 : 3	180	196.72	208.23

From the results in Figs. 3.15-3.21 and Tables 3.18-3.20, it appears that the main effect of purification of the copolymer products by extraction in hot absolute ethanol is to improve their chemical homogeneity by removal of low molecular weight oligomeric products. The DSC copolymer melting points, taken as the peak T_m rather than the onset T_m temperatures, show a general decreasing trend with increasing PEG content. This supports the NMR view that, even though the exact microstructure may not be known, the PEG does enter the copolymer structure in increasing amounts as its amount in the comonomer feed increases.

The DSC curves in Figs. 3.22-3.33 show how the melting peaks of poly(glycolic acid) and P(GA-b-PEG) vary with the conditions of synthesis and comonomer feed.

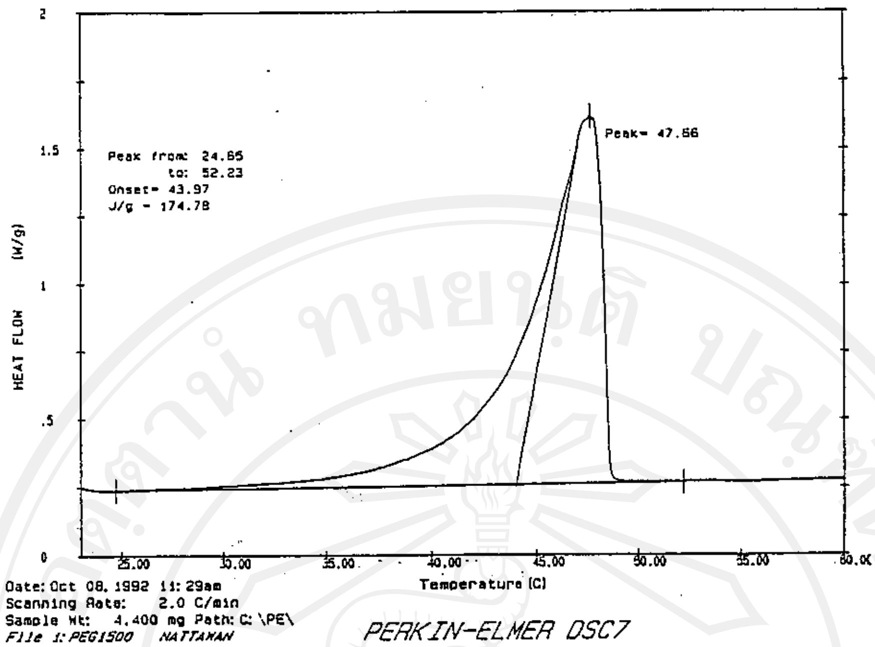

Fig. 3.22 : The DSC curve of PEG 200.

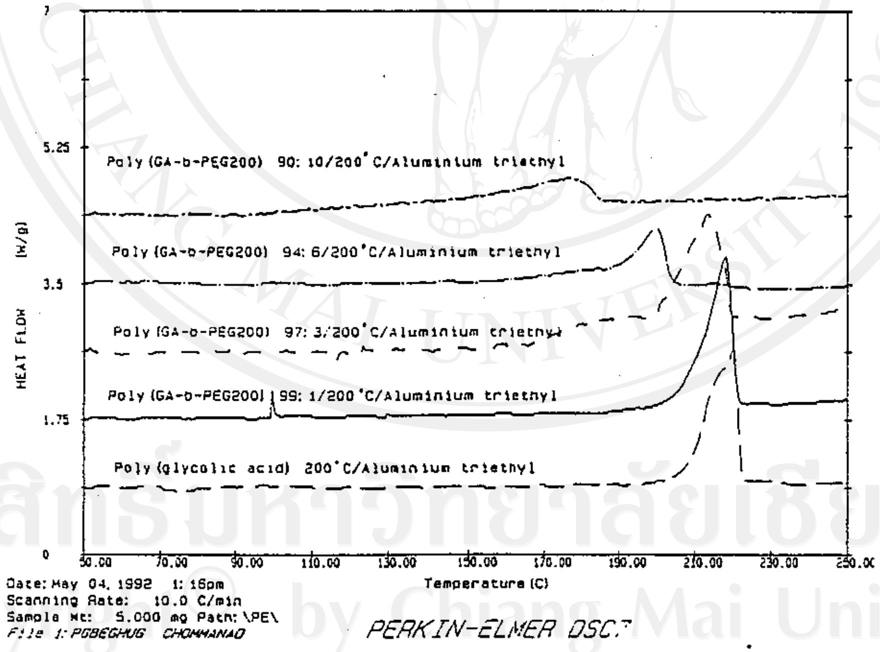

Fig. 3.23 : Comparison of the DSC curves of poly(glycolic acid) and P(GA-b-PEG 200) of various compositions synthesized at 200 °C using aluminium triethyl as initiator.

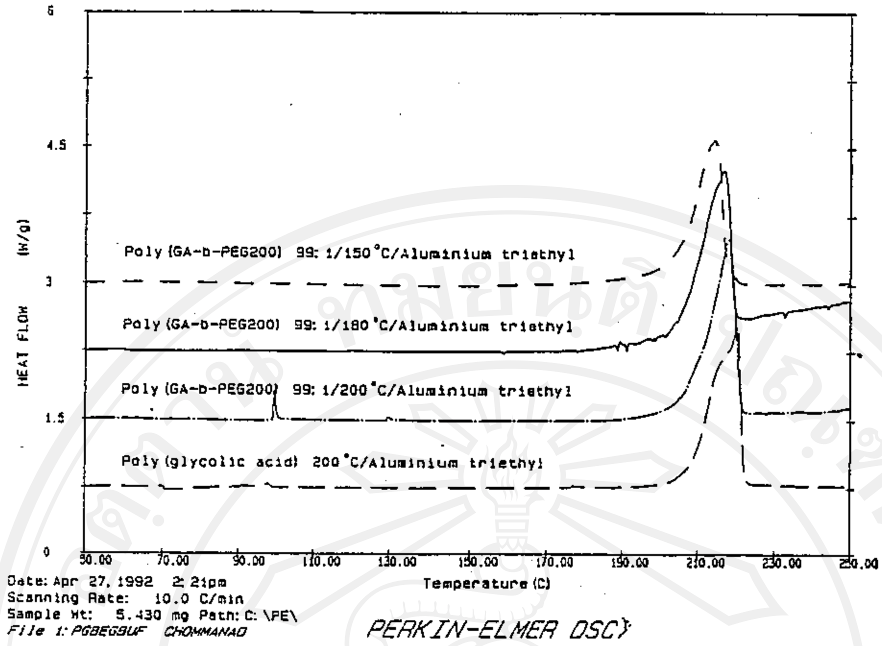

Fig. 3.24 : Comparison of the DSC curves of poly(glycolic acid) and P(GA-b-PEG 200) 99:1 synthesized at various temperature using aluminium triethyl as initiator.

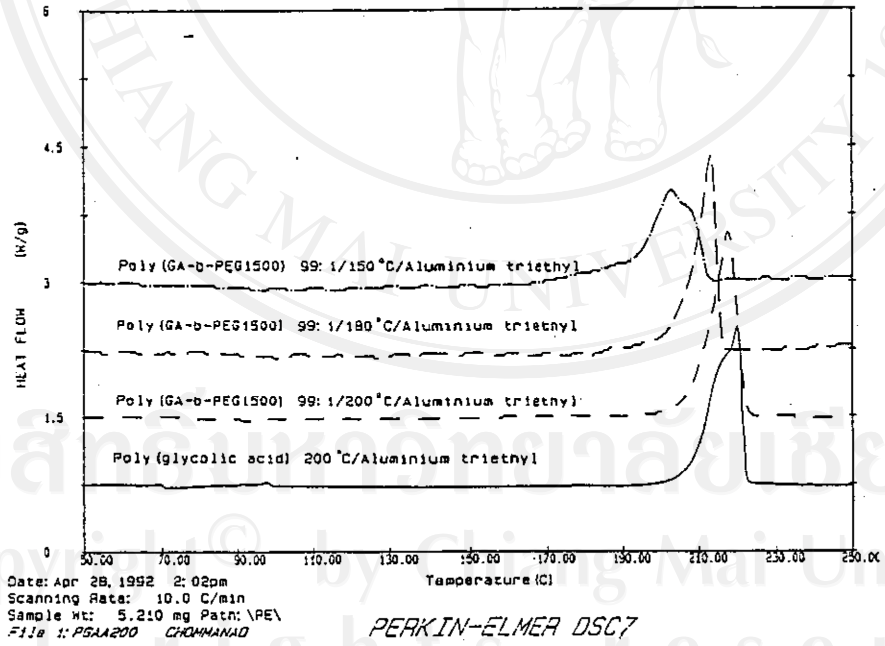

Fig. 3.25 : Comparison of the DSC curves of poly(glycolic acid) and P(GA-b-PEG 1500) 99:1 synthesized at various temperature using aluminium triethyl as initiator.

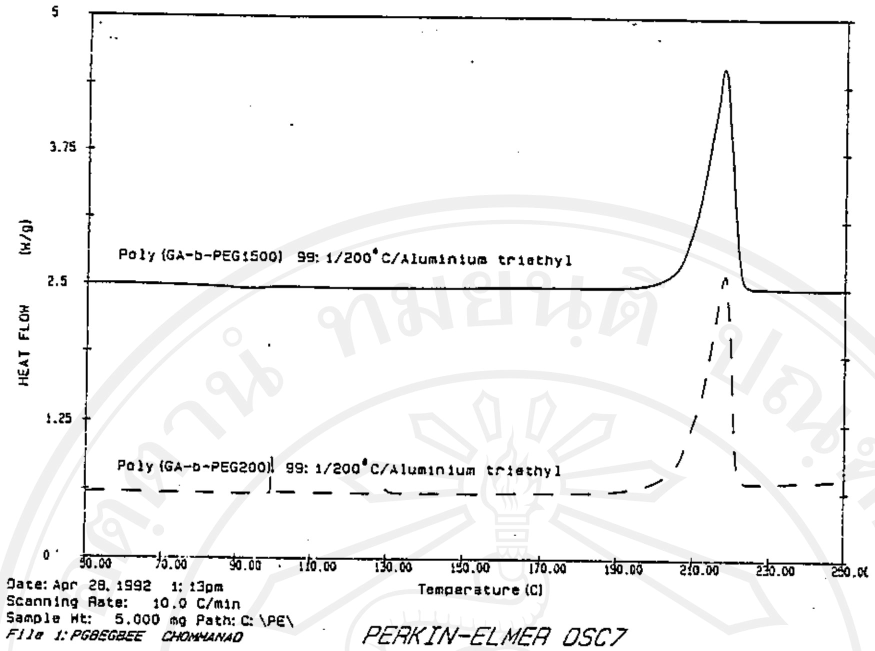

<u>Fig. 3.26</u> : **Comparison of the DSC curves of P(GA-b-PEG 200) 99:1 and P(GA-b-PEG 1500) 99:1 synthesized at 200 °C using aluminium triethyl as initiator.**

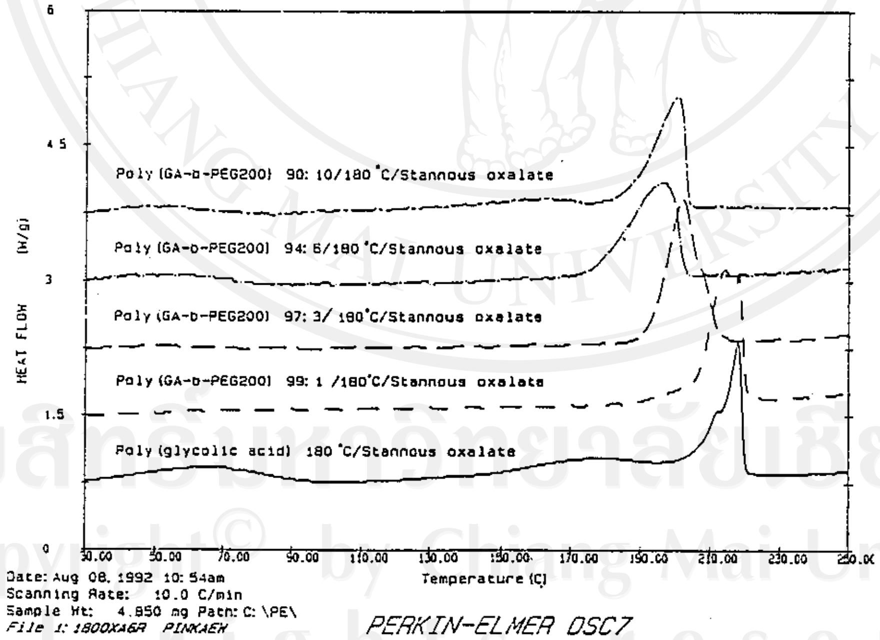

<u>Fig. 3.27</u> : **Comparison of the DSC curves of poly(glycolic acid) and P(GA-b-PEG 200) of various compositions at 180 °C using stannous oxalate as initiator.**

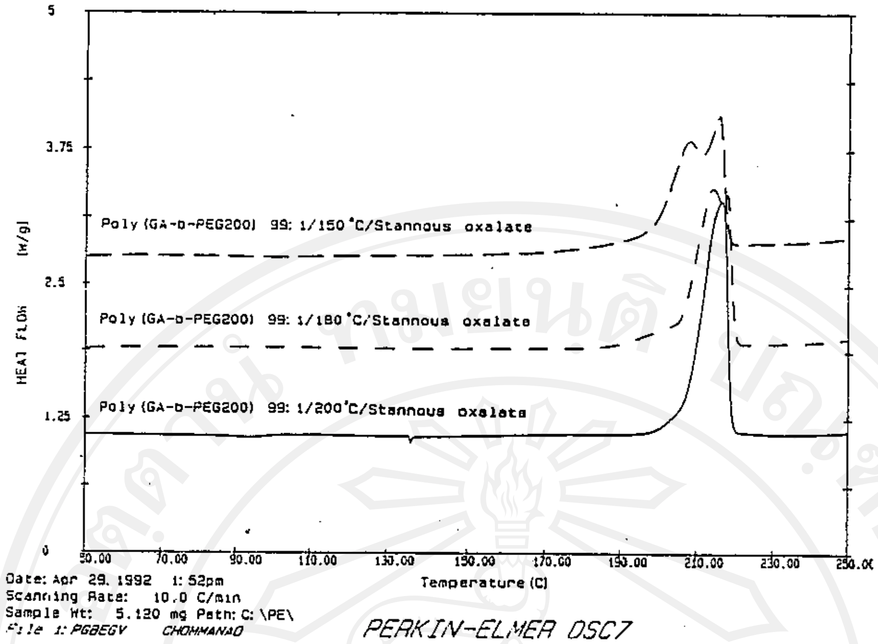

Fig. 3.28 : Comparison of the DSC curves of P(GA-b-PEG 200) 99:1 synthesized at various temperatures using stannous oxalate as initiator.

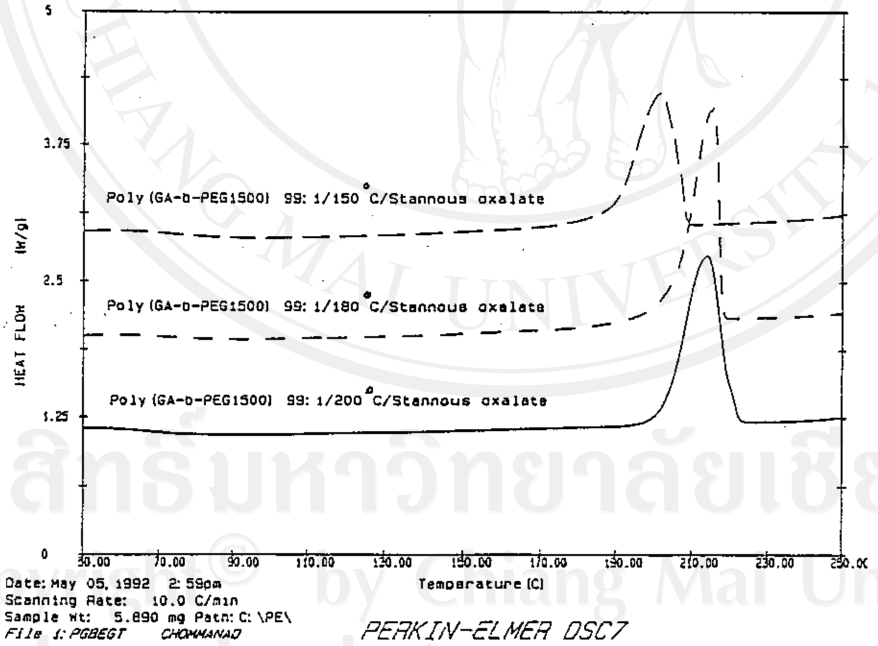

Fig. 3.29 : Comparison of the DSC curves of P(GA-b-PEG 1500) 99:1 synthesized at various temperatures using stannous oxalate as initiator.

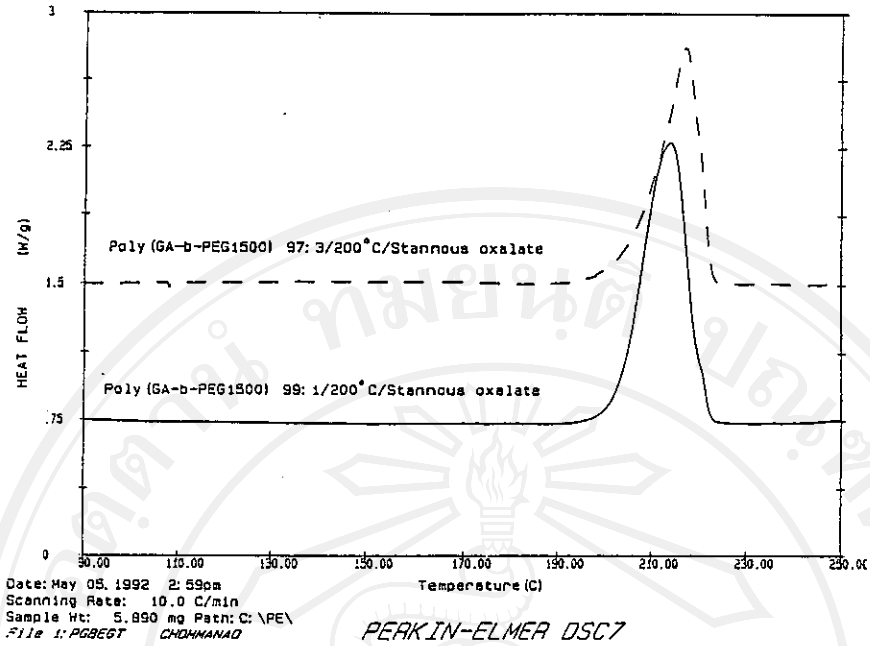

Fig. 3.30 : Comparison of the DSC curves of P(GA-b-PEG 1500) 99:1 and P(GA-b-PEG 1500) 97:3 synthesized at 200 °C using stannous oxalate as initiator.

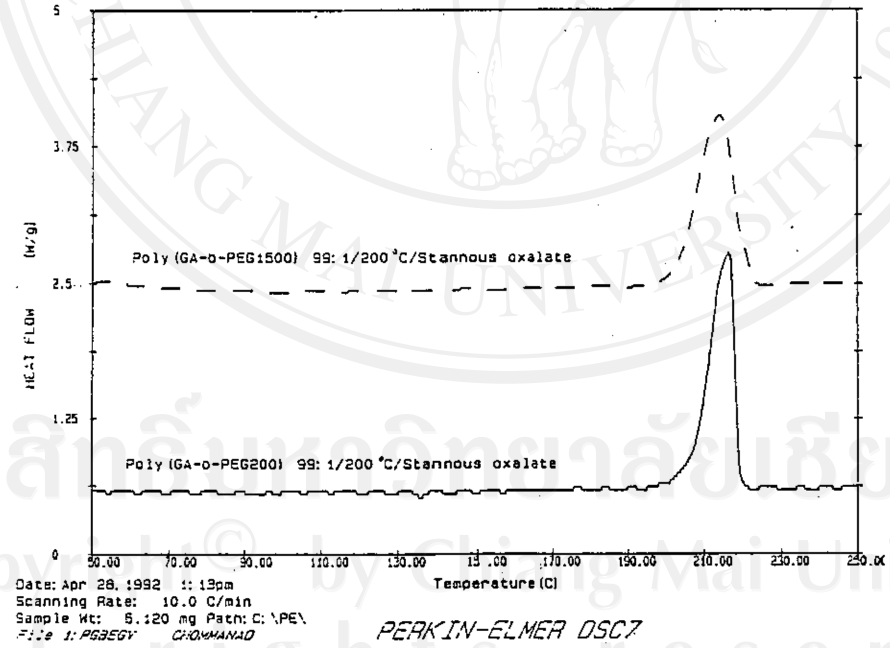

Fig. 3.31 : Comparison of the DSC curves of P(GA-b-PEG 200) 99:1 and P(GA-b-PEG 1500) 99:1 synthesized at 200 °C using stannous oxalate as initiator.

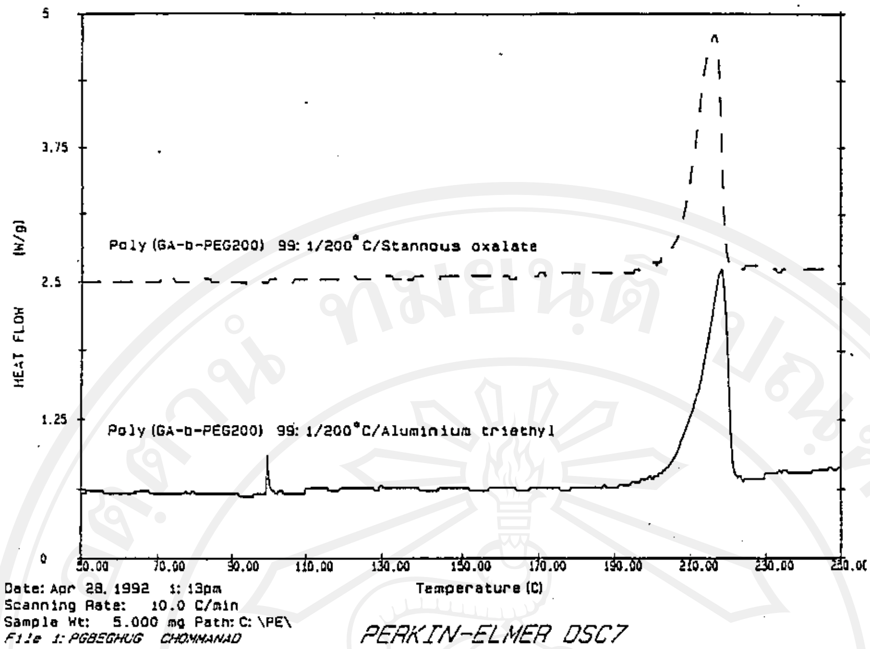

<u>Fig. 3.32</u> : Comparison of the DSC curves of (GA-b-PEG 200) 99:1 synthesized at 200 °C using different initiators.

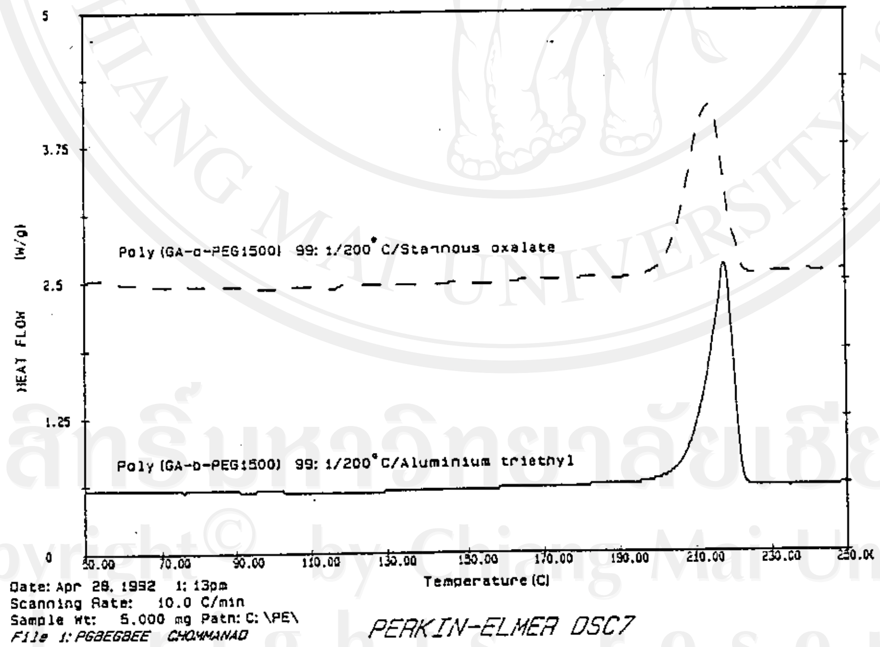

<u>Fig. 3.33</u> : Comparison of the DSC curves of P(GA-b-PEG 1500) 99:1 synthesized at 200 °C using different initiators.

Table 3.21 : Visually observed melting ranges and DSC-derived melting peak parameters for poly(glycolic acid) and P(GA-b-PEG 200) synthesized using aluminium triethyl as initiator.

Monomer Ratio (mole %)	Temp. of Copolymerisation	Melting Range (visual observation)	DSC Melting Peak Parameters *			
G : PEG 200	(°C)	(°C)	Onset (°C)	Peak (Max) (°C)	Heat of Fusion ** (J/g)	Fig./Page
100 : 0	150	205-215	211.07	220.21	93.26	-
	180	210-213	214.79	219.80	95.93	-
	200	210-219	212.17	220.08	97.04	3.23/77
99 : 1	150	200-210	204.88	218.08	97.03	3.24/78
	180	200-210	206.93	216.48	87.82	3.24/78
	200	210-213	209.01	214.24	94.11	3.24/78
97 : 3	150	192-200	191.66	201.64	93.11	-
	180	190-202	195.44	210.29	82.10	-
	200	195-207	199.73	213.32	89.35	3.23/77
94 : 6	150	150-159	158.94	185.04	84.33	-
	180	177-187	183.15	198.17	94.77	-
	200	180-192	188.98	199.64	75.36	3.23/77
90 : 10	150	150-155	149.00	175.34	65.43	-
	180	145-150	153.72	176.28	69.80	-

* data values as computed by the DSC instrument used

** heat of fusion derived from peak area (normalized) and directly proportional to the % crystallinity of the sample

Table 3.22 : Visually observed melting ranges and DSC-melting peak parameters for poly(glycolic and P(GA-b-PEG 1500) synthesized using aluminium triethyl as initiator.

Monomer Ratio (mole %)	Temp. of Copolymerisation	Melting Range (visual observation)	DSC Melting Peak Parameters *			
G : PEG 1500	(°C)	(°C)	Onset (°C)	Peak (Max) (°C)	Heat of Fusion ** (J/g)	Fig./Page
100 : 0	150	205-215	211.07	220.21	93.26	-
	180	210-213	214.79	219.80	95.93	-
	200	210-219	212.17	220.08	97.04	3.25/78
99 : 1	150	190-200	193.09	203.01	96.17	3.25/78
	180	205-210	206.06	213.26	97.10	3.25/78
	200	202-213	204.47	215.06	75.12	3.25/78
97 : 3	150	185-190	189.56	190.45	93.11	-
	180	190-197	191.46	203.85	88.75	-
	200	197-208	207.76	213.78	74.03	-

Table 3.23 : **Visually observed melting ranges and DSC-derived melting peak parameters for poly(glycolic acid) and P(GA-b-PEG 200) synthesized using stannous oxalate as initiator.**

Monomer Ratio (mole %)	Temp. of Copolymerisation	Melting Range (visual observation)	DSC Melting Peak Parameters *			
G : PEG 200	(°C)	(°C)	Onset (°C)	Peak (Max) (°C)	Heat of Fusion ** (J/g)	Fig./Page
100 : 0	150	208-218	210.36	220.35	95.36	-
	180	208-220	212.55	218.45	97.28	3.27/79
	200	211-221	212.67	220.55	98.36	-
99 : 1	150	203-209	206.25	215.32	99.22	3.28/80
	180	205-217	205.28	213.91	99.62	3.28/80
	200	209-211	207.29	216.77	104.73	3.28/80
97 : 3	150	180-191	186.25	193.37	101.91	-
	180	190-197	192.95	201.57	107.71	3.27/79
	200	204-212	200.89	211.73	105.33	-
94 : 6	150	150-165	159.70	181.97	92.98	-
	180	170-185	177.43	195.46	103.20	3.27/79
	200	200-208	196.14	206.25	89.25	-
90 : 10	150	170-173	186.26	200.18	101.69	-

Table 3.24 : Visually observed melting range and DSC-derived melting peak parameters for poly(glycolic acid) and P(GA-b-PEG 1500) synthesized using stannous oxalate as initiator.

Monomer Ratio (mole %)	Temp. of copolymerisation	Melting Range (visual observation)	DSC Melting Peak Parameters *			
G : PEG 1500	(°C)	(°C)	Onset (°C)	Peak (Max) (°C)	Heat of Fusion ** (J/g)	Fig./Page
100 : 0	150	208-218	210.36	220.35	95.36	—
	180	208-220	212.55	218.45	97.28	3.27 / 79
	200	211-221	212.67	220.55	98.36	—
99 : 1	150	196-200	289.48	201.32	96.65	3.29/80
	180	200-206	205.86	215.60	107.74	3.29/80
	200	202-210	203.11	213.91	105.68	3.29/80
97 : 3	150	165-187	160.97	179.64	100.92	—
	180	196-202	147.04	208.23	105.43	—
	200	203-209	208.07	217.13	80.72	3.30/81
94 : 6	150	170-180	169.35	177.60	85.26	—
	180	195-201	175.32	181.78	11.23	—

Table 3.25 : **DSC heats of fusion and % crystallinities of PGA synthesized under various conditions.**

Initiator	Temperature of Polymerisation (°C)	Heat of Fusion (J/g)	% Crystallinity
Aluminium triethyl	150	93.26	45.1
	180	95.93	46.4
	200	97.04	46.9
Stannous oxalate	150	95.36	46.1
	180	97.28	47.1
	200	98.36	47.6

The data in the previous Tables 3.21-3.24 compares the PGA and P(GA-b-PEG) melting ranges, as determined by visual observation, with various melting peak parameters, as derived from the previous DSC curves. From this combined data, the following conclusions can be drawn:

(1) Comparison of Methods

The melting ranges determined by visual observation correspond approximately, in the majority of cases, to the " onset ⟶ peak (max.)" range of the DSC melting peak. However, visual comparisons are often complicated by the different melting behaviours of samples of varying crystallinities/morphologies. In this respect, DSC analysis is much more reliable.

(2) Effect of Temperature

As a general trend, as the temperature of copolymerisation increased, the melting range increased. This was probably a molecular weight effect arising from the limitation imposed by premature solidification at the reaction temperature. Thus, as the temperature increased, the time for reaction in the melt state increased, leading to higher molecular weights and higher melting ranges.

(3) Effect of Mole % PEG in Comonomer Feed

As the mole % PEG in the comonomer feed increased from 1-10 %, the melting ranges of the copolymers decreased, as would be expected if there were increasing amounts of PEG in the copolymer structures.

(4) Effect of PEG Molecular Weight

Again as expected, the melting ranges of the P(GA-b-PEG 200) copolymers were higher than those of the corresponding P(GA-b-PEG 1500) copolymers synthesized under the same conditions (comonomer feed mole %, temperature, initiator). Since the PEG 1500 "soft segment" blocks are approximately 7.5 times longer than the PEG 200 blocks, they will surely exert a much greater "flexibilizing effect" on a copolymer's matrix morphology. This, in turn, would lead to an increase in molecular mobility, a looser matrix and, hence, lower onset and peak melting temperatures. It should also be noted in Tables 3.22 and 3.24 that, in the case of PEG 1500, copolymerisation to a solid product was only possible up to a certain limit of PEG 1500 in the comonomer feed. Above this limit, the copolymer was obtained in the form of a viscous liquid, even after prolonged (> 15 hours) heating.

(5) Effect of Initiator

On comparing the two initiators used, aluminium triethyl and stannous oxalate, there is no clear indication that either one is more effective than the other. The melting ranges of copolymers obtained under the same conditions but with different initiators are, with a few exceptions, very similar in value. However, where differences do exist, the aluminium triethyl-initiated copolymer tended to the slightly higher melting range. Not shown in the tables but worthy of mention is the observation that the apparent rates of reaction, as compared in terms of the times taken to solidify, were also quite similar for the two initiators studied.

(6) Heats of Fusion

The heats of fusion given in Tables 3.21-3.24 are computed from the normalized DSC melting peak areas. They are directly related to the % crystallinities of the samples. From the results, it is difficult to draw any firm conclusions about the effects of the various synthesis variables on polymer crystallinity. Quantitative comparisons of heats of fusion are usually restricted to samples of the same polymer which differ in only a single aspect of synthesis or thermal history. To calculate the % crystallinity of a sample from its heat of fusion, a reference value for the heat of fusion of a theoretical 100 % crystalline sample must be known, usually from the tables of data available in the "Polymer Handbook" [25]. For the polymers/copolymers studied here, only the value for poly(glycolic acid) is listed; consequently, the % crystallinity can only be calculated for this polymer. The DSC heats of fusion and corresponding % crystallinities of the PGA synthesized here under various conditions are shown in Table 3.24. Their similarities indicate that the % crystallinity was not significantly affected by either the initiator or reaction temperature employed.

Sample Calculation:

From the "Polymer Handbook" [25], heat of fusion of a theoretically 100 % crystalline sample (ΔH_f^*) of PGA = 12 kJ/mole

where, mole = molecular weight of repeat unit in g

= 58.04 g

i.e., ΔH_f^* = 12 kJ/58.04 g

From Table 3.24 the experimental heat of fusion (ΔH_f) of PGA synthesized using aluminium triethyl as initiator at 150 °C was deterimined as:

$$\Delta H_f = 93.26 \text{ J/g}$$

Therefore, % crystallinity $= \dfrac{\Delta H_f}{\Delta H_f^*} \times 100\ \%$

$$= \frac{93.26 \times 58.04}{12000} \times 100\ \%$$

$$= 45.1\ \%$$

This and the other values in Table 3.25 are of the same order as commercial PGA sold in the form of absorbable surgical sutures (trade name "Dexon": Davis & Geck, American Cyanamid) which is usually claimed to have a % crystallinity of about 50 %. This slightly higher value is probably due to the additional crystallisation which is induced by drawing of the fibres during melt spinning.

3.6 Thermogravimetry (TG)

Thermogravimetry (TG) is a technique in which the mass of a substance is measured as a function of temperature while the substance is subjected to a controlled temperature program. There are two types of thermogravimetry: (a) isothermal thermogravimetry, in which the procedure is to record the change in weight of the sample as a function of time at constant temperature, and (b) non-isothermal (dynamic) thermogravimetry, in which the change in weight of the sample is recorded as a function of both temperature and time as its temperature is raised at a constant heating rate.

In this project, the thermal stabilities of polymer/copolymer samples were compared by means of dynamic thermogravimetry using a Stanton Thermobalance Model TR-1.

3.6.1 Analytical Procedure

For dynamic TG analysis, a weighed amount of sample was placed in a silica crucible and heated in an inert nitrogen atmosphere employing the following conditions:

initial sample weight : 80 mg (approx.)
atmosphere : N_2 (dry, O_2-free)
N_2 flow-rate : 100 ml/min (downflow)
chart speed : 12 ins/hr
heating rate : 4 °C/min
temperature range : ambient - end of decomposition

3.6.2 Results

A typical set of results is shown in Table 3.26 and Fig. 3.34 from which it can be seen that PGA initially begins to lose weight at about 220 °C with weight loss complete at about 390 °C.

The other TG curves which follow in Figs. 3.35-3.51 compare the thermal degradation characteristics of selected combinations of the PGA and P(GA-b-PEG) samples synthesized in this project.

Table 3.26 : Dynamic TG data for PGA synthesized at 180 °C using stannous oxalate as initiator.

Temperature (°C)	Weight (mg)	Temperature (°C)	Weight (mg)
80	80	280	52
100	80	290	48
120	80	300	41
140	80	310	27
160	80	320	25
180	80	330	23
200	80	340	16
210	80	350	9
220	79	360	9
230	78	370	6
240	76	380	5
250	68	390	2
260	65	400	2
270	54		

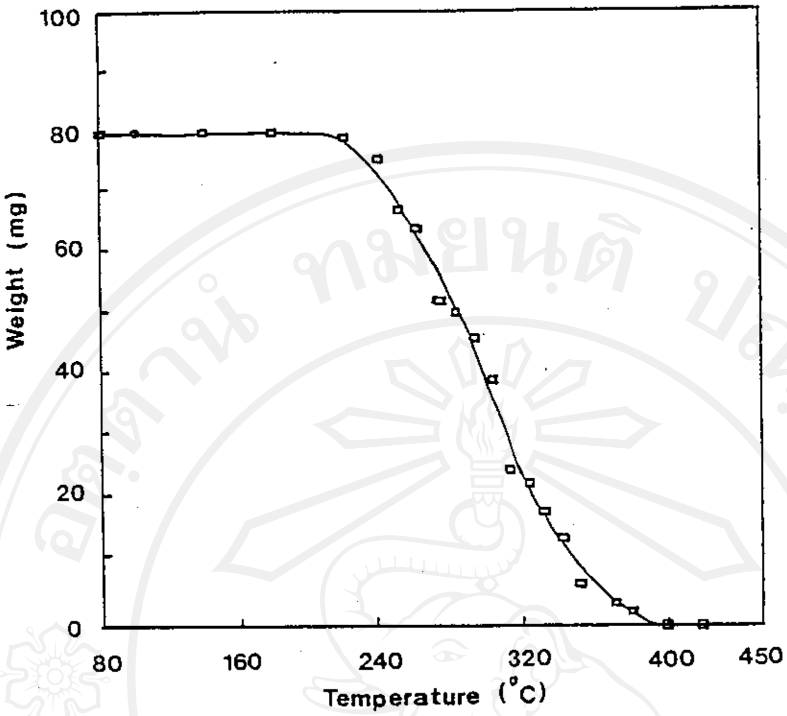

Fig. 3.34 : Dynamic TG curve for PGA synthesized at 180 °C using stannous oxalate as initiator.

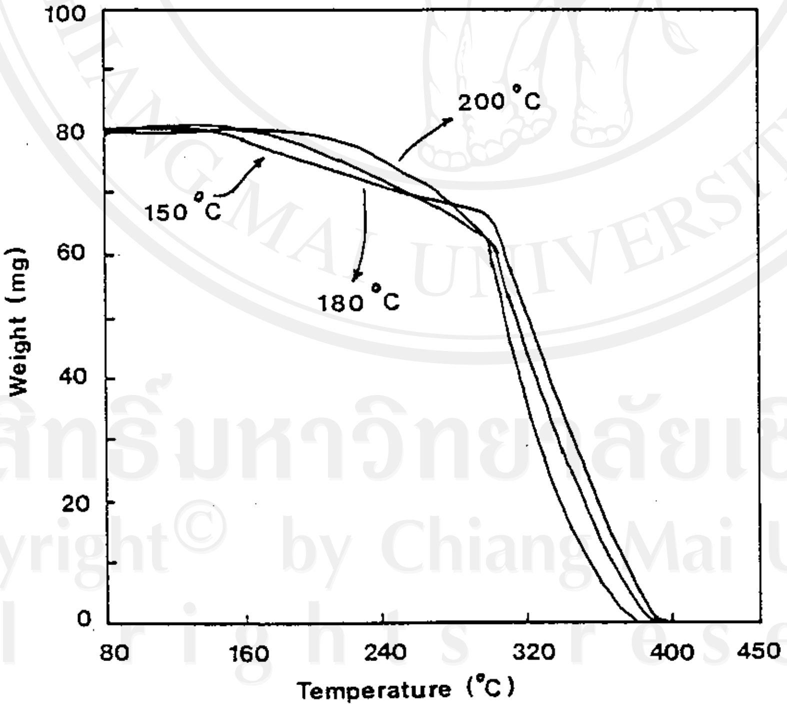

Fig. 3.35 : Comparison of the TG curves of PGA synthesized at various temperatures using aluminium triethyl as initiator.

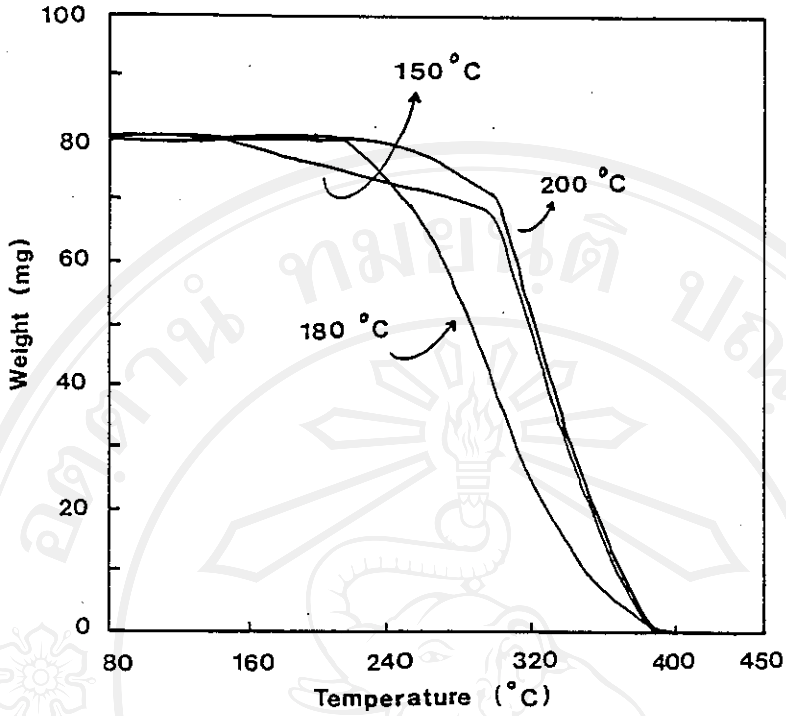

Fig. 3.36 : Comparison of the TG curves of PGA synthesized at various temperatures using stannous oxalate as initiator.

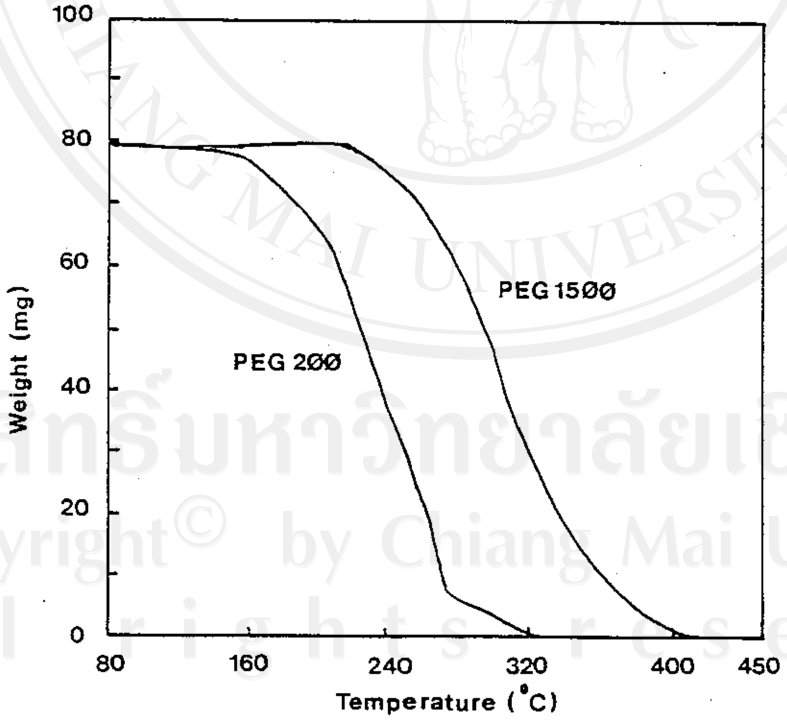

Fig. 3.37 : Comparison of the TG curves of PEG of different molecular wieghts.

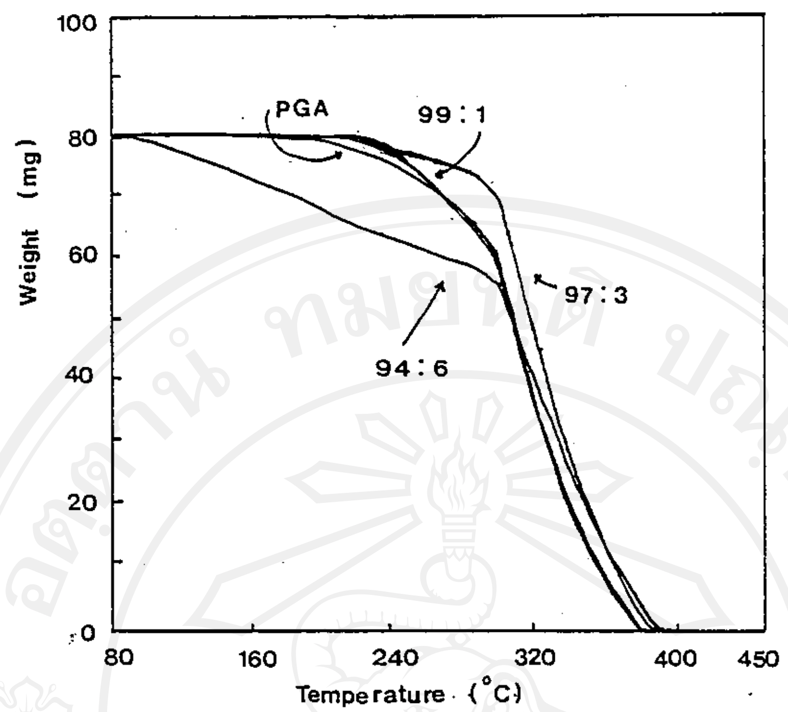

Fig. 3.38 : Comparison of the TG curves of PGA and P(GA-b-PEG 200) of various compositions synthesized at 200 °C using aluminium triethyl as initiator.

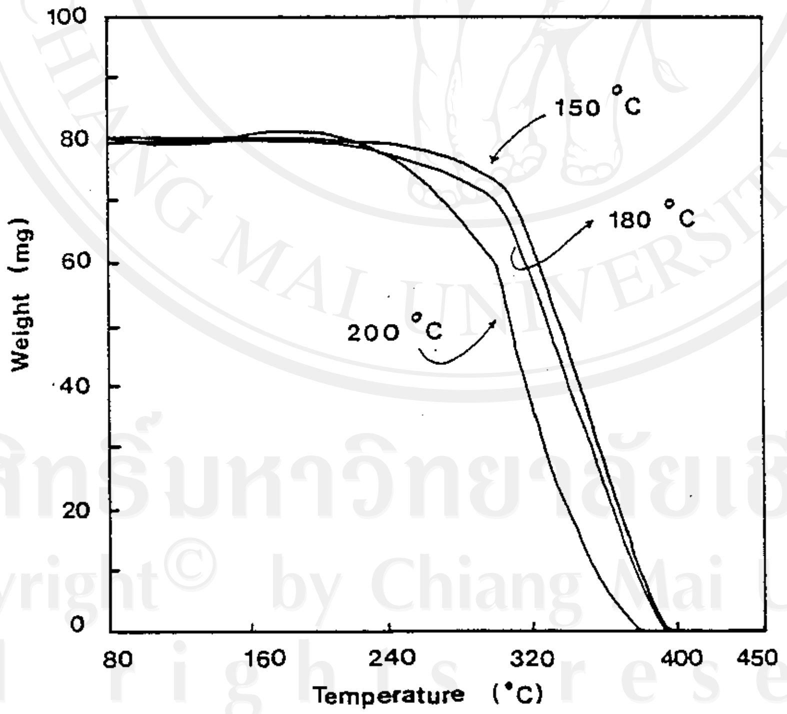

Fig. 3.39 : Comparison of the TG curves of P(GA-b-PEG 200) 99:1 synthesized at various temperatures using aluminium triethyl as initiator.

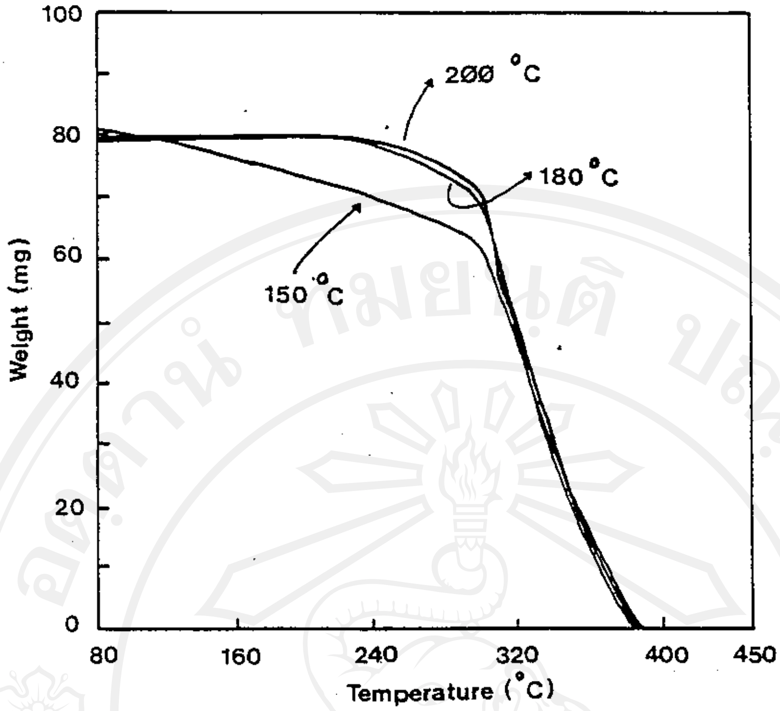

Fig. 3.40 : Comparison of the TG curves of P(GA-b-PEG 200) 97:3 synthesized at various temperatures using aluminium triethyl as initiator.

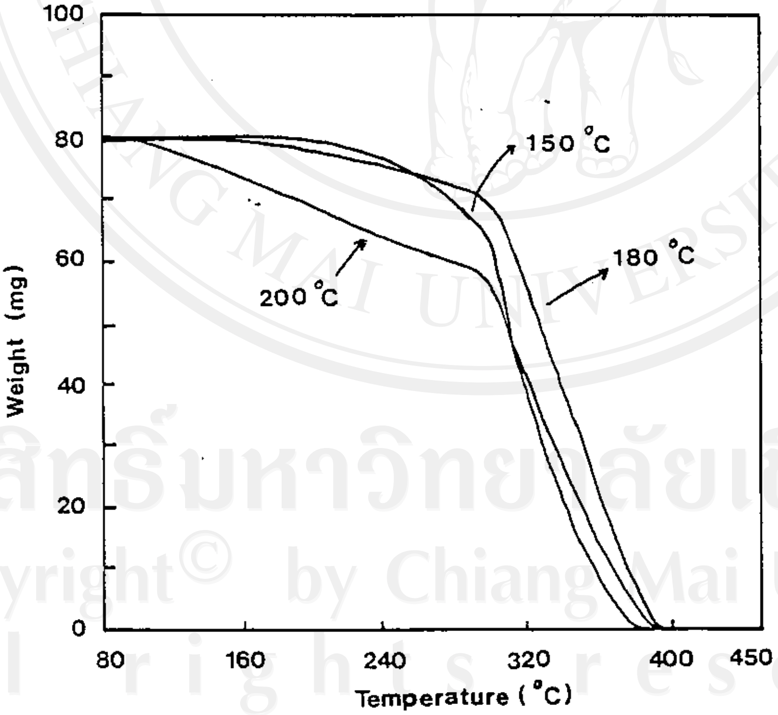

Fig. 3.41 : Comparison of the TG curves of P(GA-b-PEG 200) 94:6 synthesized at various temperatures using aluminium triethyl as initiator.

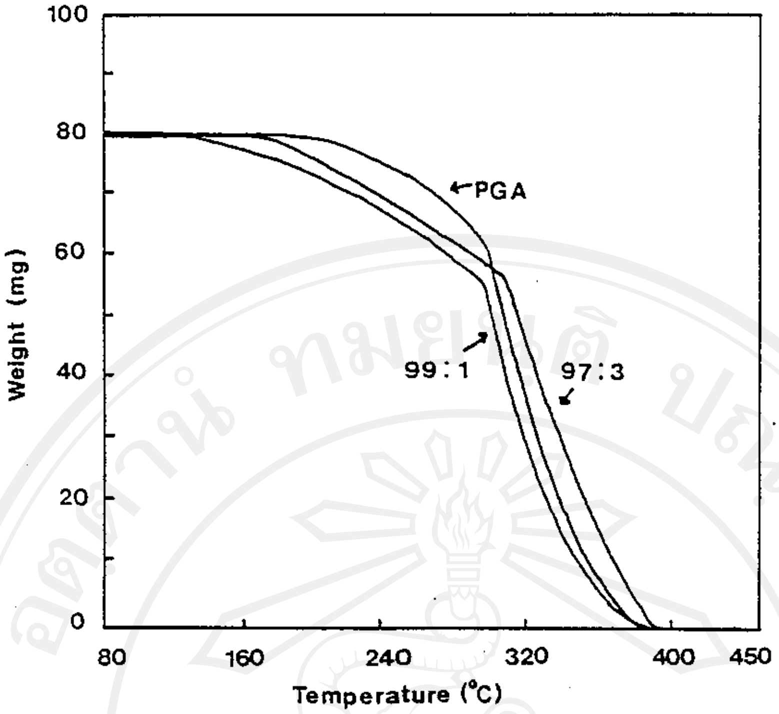

Fig. 3.42 : Comparison of the TG curves of PGA and P(GA-b-PEG 1500) of various compositions synthesized at 200 °C using aluminium triethyl as initiator.

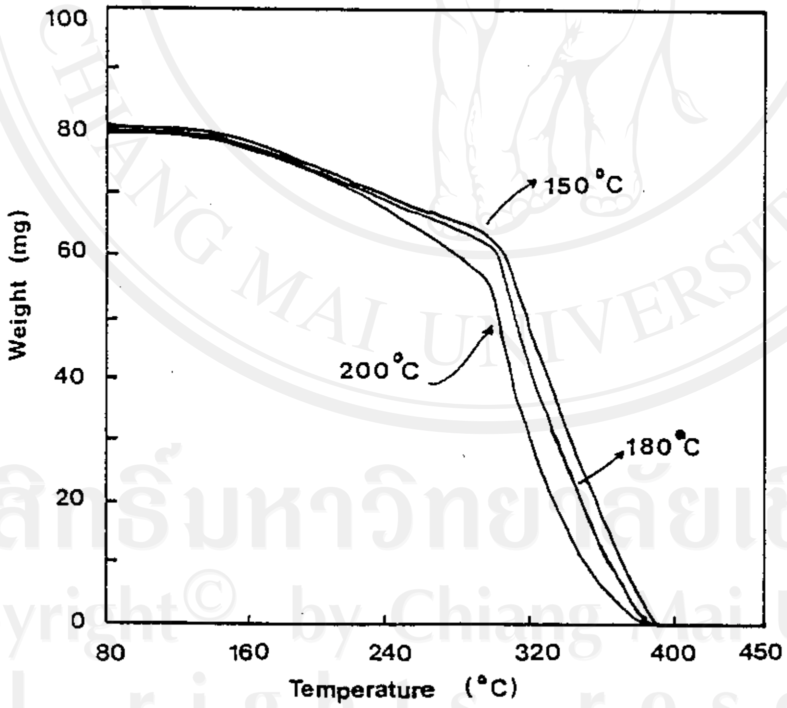

Fig. 3.43 : Comparison of the TG curves of P(GA-b-PEG 1500) 99:1 synthesized at various temperatures using aluminium triethyl as initiator.

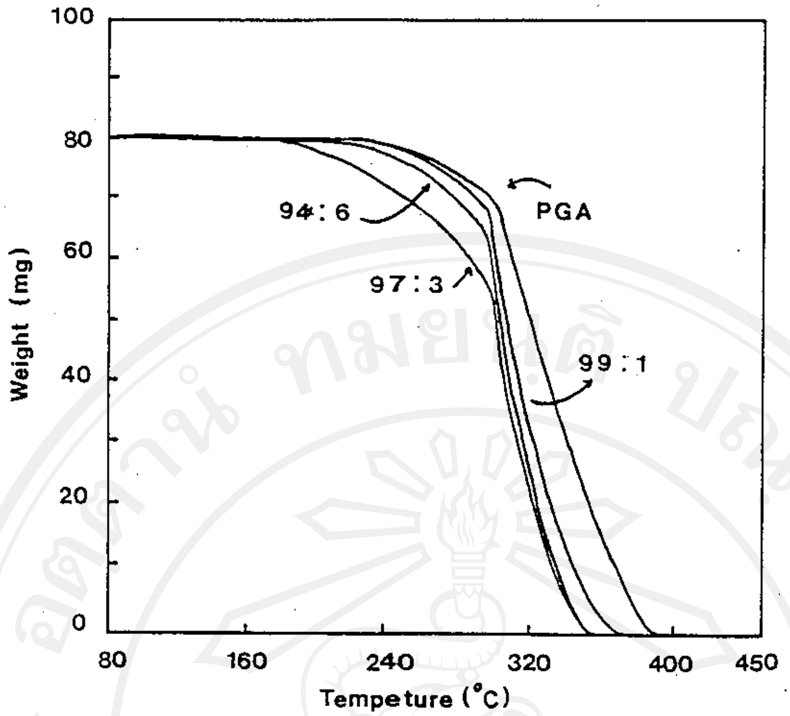

Fig. 3.44 : Comparison of the TG curves of PGA and P(GA-b-PEG 200) of various compositions synthesized at 200 °C using stannous oxalate as initiator.

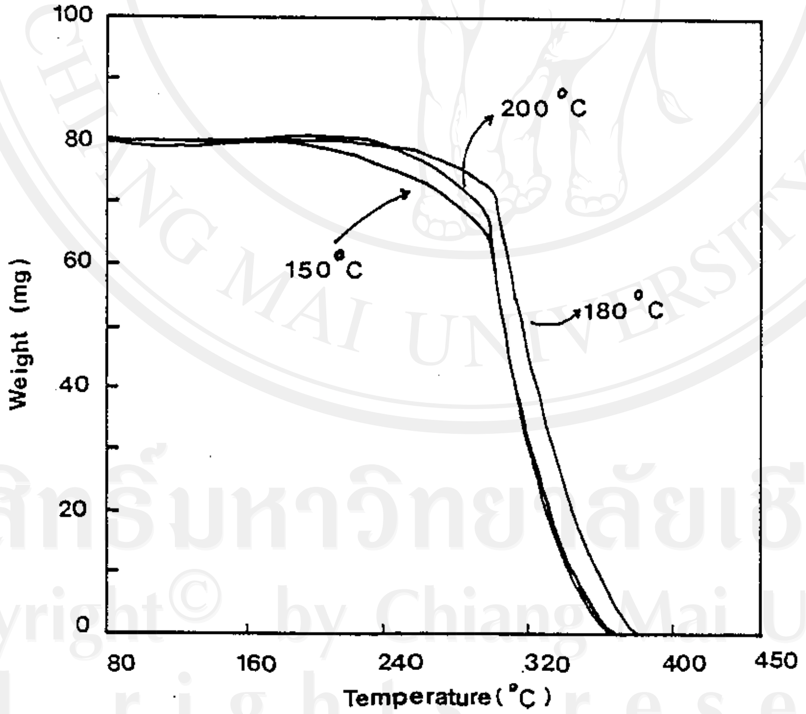

Fig. 3.45 : Comparison of the TG curves of P(GA-b-PEG 200) 99:1 synthesized at various temperatures using stannous oxalate as initiator.

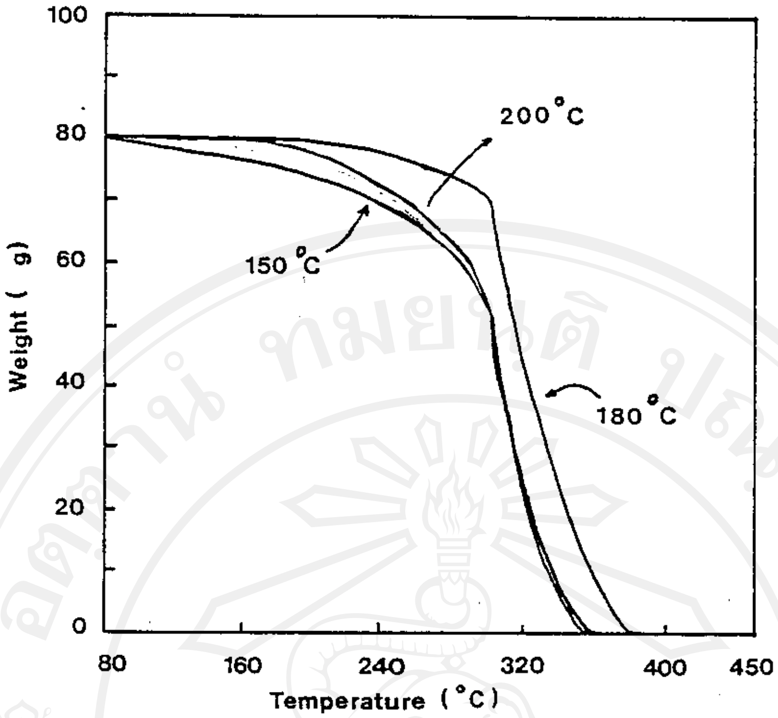

Fig. 3.46 : Comparison of the TG curves of P(GA-b-PEG 200) 97:3 synthesized at various temperatures using stannous oxalate as initiator.

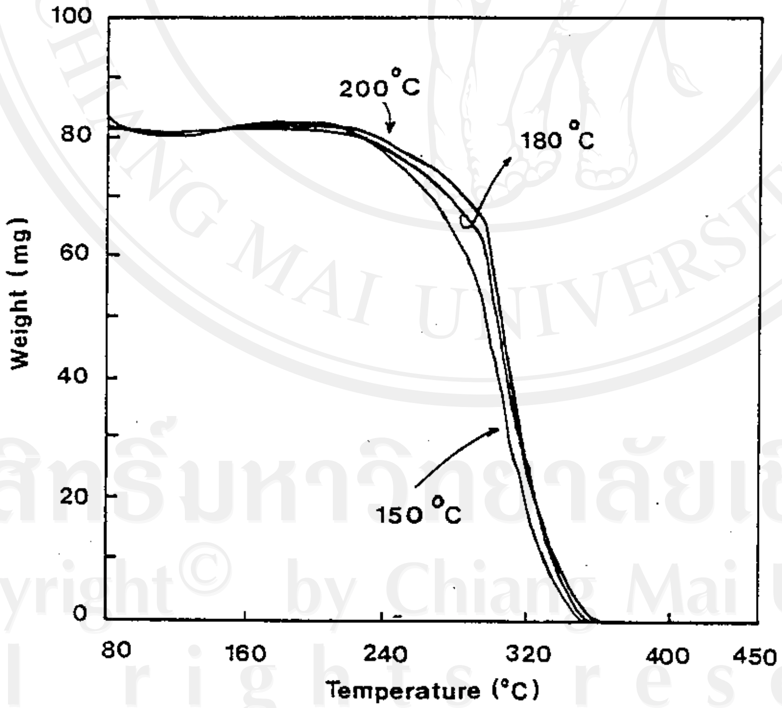

Fig. 3.47 : Comparison of the TG curves of P(GA-b-PEG 200) 94:6 synthesized at various temperatures using stannous oxalate as initiator.

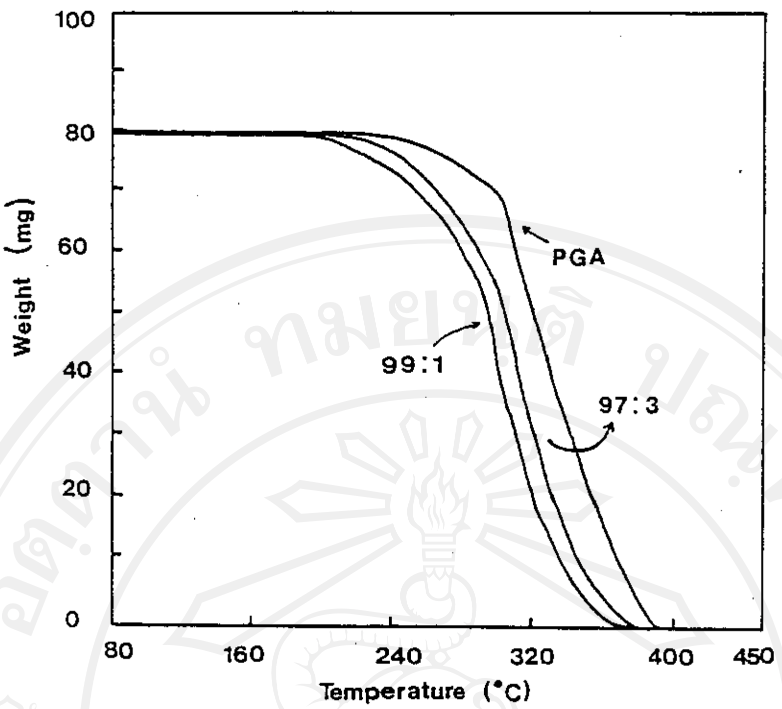

Fig. 3.48 : Comparison of the TG curves of PGA and P(GA-b-PEG 1500) of various compositions synthesized at 200 °C using stannous oxalate as initiator.

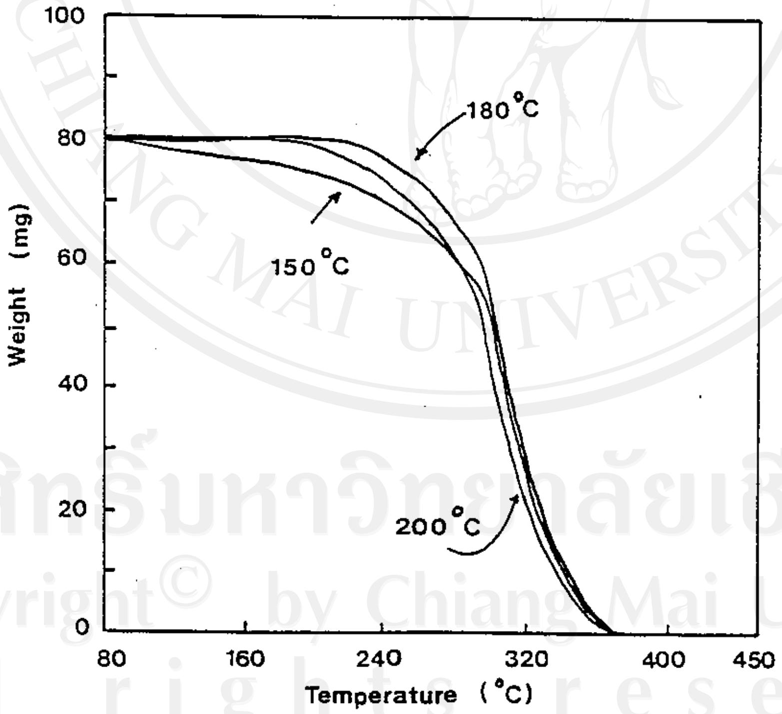

Fig. 3.49 : Comparison of the TG curves of P(GA-b-PEG 1500) 99:1 synthesized at various temperatures using stannous oxalate as initiator.

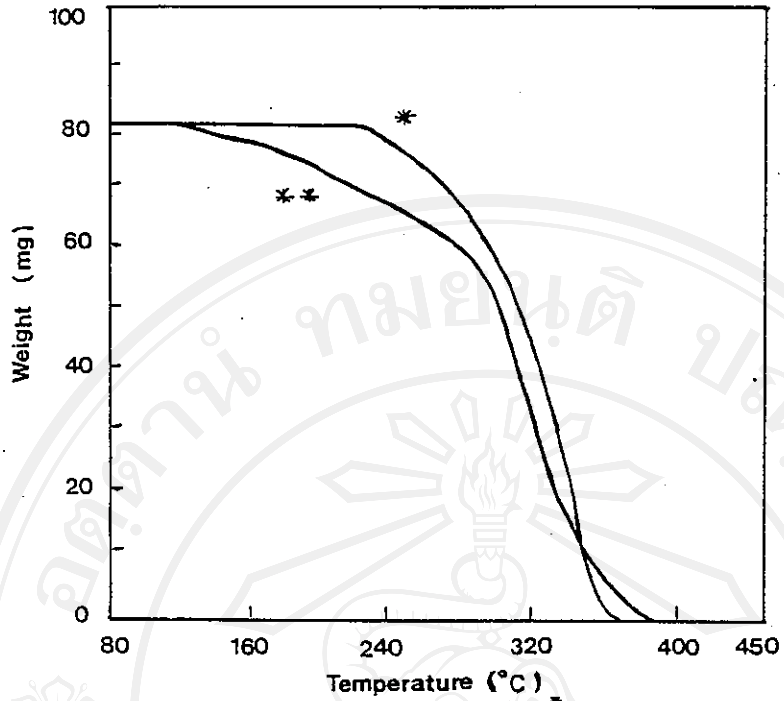

Fig. 3.50 : Comparison of the TG curves of *P(GA-b-PEG 200) 99:1 and **P(GA-b-PEG 1500) 99:1 synthesized at 200 °C using aluminium triethyl as initiator.

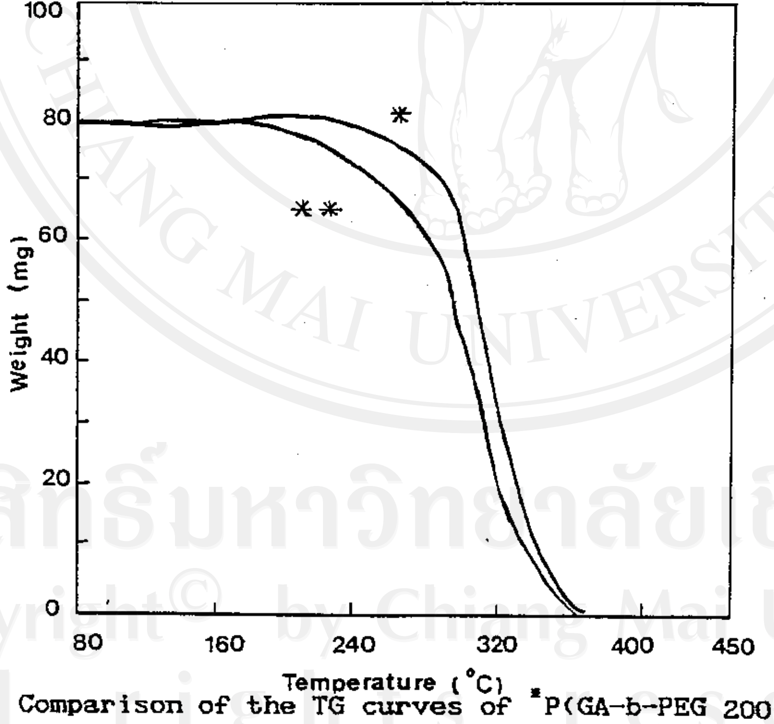

Fig. 3.51 : Comparison of the TG curves of *P(GA-b-PEG 200) 99:1 and **P(GA-b-PEG 1500) 99:1 synthesized at 200 °C using stannous oxalate as initiator.

Table 3.27 : **The melting and thermal degradation ranges of Poly(glycolic acid), poly(ethylene glycol) and P(GA-b-PEG 200) using aluminium triethyl as initiator.**

Monomer ratio (mole %)	Temperature of copolymerisation	Temperature Range		ΔT^{***}
G : PEG 200	(°C)	T_m * (°C)	T_d ** (°C)	(°C)
100 : 0	150	211-220	160-380	-60
	180	214-219	200-380	-19
	200	212-220	210-380	-10
0 : 100	-	-	100-260	-
99 : 1	150	204-214	210-370	-4
	180	206-216	210-370	-6
	200	209-218	230-360	12
97 : 3	150	191-201	100-370	-101
	180	195-210	210-360	0
	200	199-213	230-370	17

Table 3.27 : (continued)

Monomer ratio (mole %) G : PEG 200	Temperature of copolymerisation (°C)	Temperature Range		ΔT *** (°C)
		T_m * (°C)	T_d ** (°C)	
94 : 6	150	158-185	160-360	-25
	180	183-198	160-370	-38
	200	188-199	100-370	-99
90 : 10	150	149-175	120-360	-55
	180	153-176	120-360	-56

* obtained from DSC

** obtained from TG

*** ΔT calculated as the difference between the lower limit of the T_d range and the upper limit of the T_m range

i.e., $\Delta T = T_d\,(\text{min}) - T_m\,(\text{max})$

This T value can be considered as an indicator of the width of the polymer's processing stability range for melt spinning, the process normally used for the spinning of monofilament fibres for use as surgical sutures.

Table 3.28 : **The melting and thermal degradation ranges of poly(glycolic acid), poly(ethylene glycol) and P(GA-b-PEG 1500) using aluminium triethyl as initiator.**

Monomer ratio (mole %) G : PEG 1500	Temperature of copolymerisation (°C)	Temperature Range		ΔT^{***} (°C)
		T_m * (°C)	T_d ** (°C)	
100 : 0	150	211-220	160-380	-60
	180	214-219	200-380	-19
	200	212-220	210-380	-10
0 : 100	-	-	160-360	-
99 : 1	150	193-203	120-380	-83
	180	206-213	140-360	-73
	200	204-215	140-370	-75
97 : 3	150	189-190	140-320	-50
	180	191-203	160-370	-43
	200	207-213	180-370	-33

$$\Delta T = T_d\ (\text{min}) - T_m\ (\text{max})$$

Table 3.29 : **The melting and thermal degradation ranges of poly(glycolic acid), poly(ethylene glycol) and P(GA-b-PEG 200) using stannous oxalate as initiator.**

Monomer ratio (mole %) G : PEG 200	Temperature of copolymerisation (°C)	Temperature Range		Δ T*** (°C)
		T_m * (°C)	T_d ** (°C)	
100 : 0	150	210-220	160-380	-60
	180	212-218	210-380	-8
	200	212-220	230-380	10
0 : 100	-	-	100-260	-
99 : 1	150	206-215	160-340	-55
	180	205-213	220-350	7
	200	207-216	230-350	14
97 : 3	150	186-193	100-350	-93
	180	192-201	180-360	-21
	200	200-211	180-340	-31

Table 3.29 : (continued)

Monomer ratio (mole %) G : PEG 200	Temperature of copolymerisation ($^{\circ}C$)	Temperature Range		ΔT^{***} ($^{\circ}C$)
		T_m^{*} ($^{\circ}C$)	T_d^{**} ($^{\circ}C$)	
94 : 6	150 180 200	159-181 177-195 196-206	200-340 180-340 200-340	19 -15 -6
90 : 10	150 180	186-200 145-174	120-360 140-360	-80 -34

$\Delta T = T_d\ (\text{min}) - T_m\ (\text{max})$

Table 3.30 : The melting and thermal degradation ranges of poly(glycolic acid), poly(ethylene glycol) and P(GA-b-PEG 1500) using stannous oxalate as initiator.

Monomer ratio (mole %) G : PEG 1500	Temperature of copolymerisation (°C)	Temperature Range		Δ T*** (°C)
		T_m* (°C)	T_d** (°C)	
100 : 0	150	210-220	160-380	-60
	180	212-218	210-380	-8
	200	212-220	230-380	10
0 : 100	-	-	160-360	-
99 : 1	150	189-201	100-370	-101
	180	205-215	160-360	-55
	200	203-213	160-370	-53
97 : 3	150	160-179	140-370	-39
	180	197-208	120-380	-88
	200	208-217	200-370	-17

$$\Delta T = T_d\ (\text{min}) - T_m\ (\text{max})$$

From the data in Tables 3.27-3.30, the following conclusions can be drawn:

(1) Effect of Temperature

As the temperature of copolymerisation increased, the degradation temperature range also increased. This was probably a molecular weight effect since, as the temperature increased, the time for reaction in the melt state increased, leading to higher molecular weights and higher degradation temperature ranges. It is generally the case in linear aliphatic polyesters that low molecular weight fractions decrease the initial decomposition temperature of the polymer, although have little effect on the upper limit of the decomposition range.

(2) Effect of Mole % PEG in Comonomer Feed

At the same copolymerisation temperature, as the mole % PEG in the comonomer feed increased from 1-10 %, the initial degradation temperature decreased while the final temperature remained approximately constant. This was to be expected if the PEG content of the copolymer increased, since the initial thermal decomposition temperature of PEG is considerably lower than that of PGA. It is also interesting to note that the initial T_d of P(GA-co-PEG 200/1500) is generally higher than that of PEG 200/1500 alone, a fact which suggests that the interconnecting PGA blocks exert a stabilizing effect on the PEG blocks.

(3) Effect of PEG Molecular Weight

The degradation ranges of the P(GA-b-PEG 200) copolymers were higher than those of the corresponding P(GA-b-PEG 1500) copolymers synthesized under the same conditions. Again, this is not surprising because the PEG 1500 "soft segment" blocks are approximately 7.5 times longer than those of PEG 200. They will also exert a much greater "flexibilizing effect" on a copolymer's matrix morphology so that the intermolecular forces and, hence, the temperature required to overcome the energy barriers for chain scission will be reduced.

(4) Effect of Initiator

On comparing the two initiators used, aluminium triethyl and stannous oxalate, there is no clear indication that either one is more effective than the other. The degradation ranges of copolymers obtained under the same conditions but with different initiators are seen to be very similar.

(5) Significance of ΔT

The ΔT value was calculated as the difference between the lower limit of the T_d range and the upper limit of the T_m range, so that it could be considered as an indicator of the width of the polymer's processing stability range for melt spinning. Hence, ΔT should be a positive value of at least 20-30 °C. However, almost all of the synthesized copolymers showed a negative ΔT value, thus making them unsuitable in their present form for the melt spinning process. Even those few positive ΔT copolymers showed a $\Delta T < 30$ °C which would necessitate extremely careful temperature control in the melt spinning process. This highlights a problem which needs to be solved in future research.

Introducing flexible blocks into a copolymer chain may create new problems for melt processing if the T_d of the less stable component (PEG) is below the T_m of the more stable one (PGA). On the other hand, if the copolymer is to be used in an application for which melt processing is unnecessary, such as a drug delivery matrix, this problem does not arise.

In general, the results in Tables 3.27-3.30 show that the copolymers have very wide decomposition temperature ranges over which weight loss occurs. Some of the copolymers exhibit quite distinct two-stage reactions with the transition occurring in the region of about 240-260 °C. It seems likely that the first-stage weight loss (120-220 °C) is due to a combination of both PEG block and low molecular weight (oligomeric) PGA decomposition. The major second-stage weight loss (250-380 °C) is solely due to higher molecular weight PGA and is comparable with the decomposition range of commercial "DEXON" PGA sutures (240-400 °C) [26].

3.7 Dilute-Solution Viscometry

3.7.1 General Introduction [27,28]

The ability of polymers, in general, to increase the viscosities of solvents is one of their most significant properties. The viscous drag created by the presence of random-coil polymer molecules in a flowing solvent is a measure of the size, not the mass, of the molecules. Provided that it is known that the polymer is linear rather than branched, empirical relationships can be developed between the solution viscosity and the average molecular weight of the polymer.

One of the implest ethods of examining this effect is by capillary viscometry. The most commonly used viscometers are of the Ostwald and Ubbelohde types, as shown below.

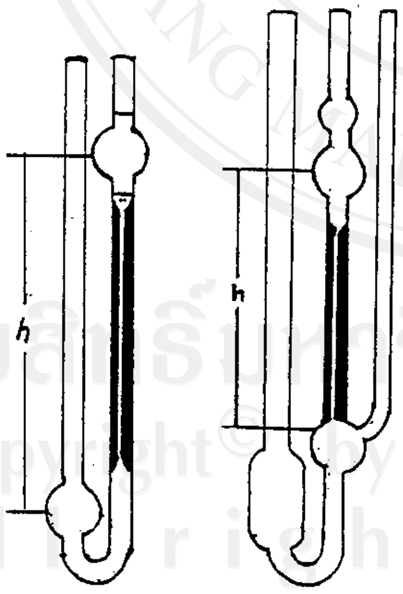

Ostwald viscometer

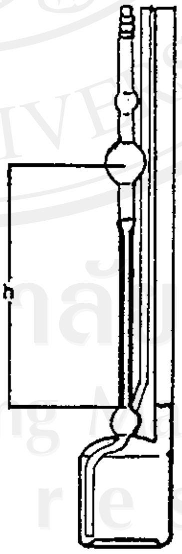

Ubbelohde viscometer

3.7.2 Determination of Intrinsic Viscosity

(a) Huggins-Kraemer Double Extrapolation Method

The intrinsic viscosity, $[\eta]$, of a polymer is most commonly determined via a combination of the Huggins Equation

$$\eta_{red} = \eta_{sp}/c = [\eta] + k'[\eta]^2c \qquad (3.11)$$

and the Kraemer Equation

$$\eta_{inh} = (\ln \eta_{rel})/c = [\eta] + k''[\eta]^2c \qquad (3.12)$$

where:

η_{red} = η_{sp}/c = reduced viscosity

η_{inh} = $(\ln \eta_{rel})/c$ = inherent viscosity

η_{rel} = t/t_o = relative viscosity

η_{sp} = $(t-t_o)/t_o$ = specific viscosity

t, t_o = flow-times of the polymer solution and pure solvent respectively

c = concentration of polymer solution in $g.dl^{-1}$

Also in these Huggins and Kraemer Equations:

k' and k" are physical interaction constants for a given polymer in a given solvent at a given temperature and are themselves related by the equation

$$k' - k'' = 0.5 \qquad (3.13)$$

The value of k' is usually in the range $0.3 < k' < 0.5$ and increases as solvent power decreases.

$[\eta]$ is the so-called "intrinsic viscosity" at infinite dilution ($c = 0$), as given by

$$[\eta] = \lim_{c \to 0} \left[\frac{\eta_{sp}}{c} \right] = \lim_{c \to 0} \left[\frac{\ln \eta_{rel}}{c} \right]$$

Consequently, it has become standard practice in dilute-solution viscometry to determine both the reduced and inherent viscosities, η_{sp}/c and $(\ln \eta_{rel})/c$, over a range of concentrations, c, and to extrapolate their values back to their common intercept, $[\eta]$, at $c = 0$.

Both η_{sp}/c and $(\ln \eta_{rel})/c$ give reasonable straight lines when plotted against c at low concentrations. The plot of $(\ln \eta_{rel})/c$ usually gives a line of small negative slope while the corresponding η_{sp}/c plot has a larger positive slope, as shown in Fig. 3.52.

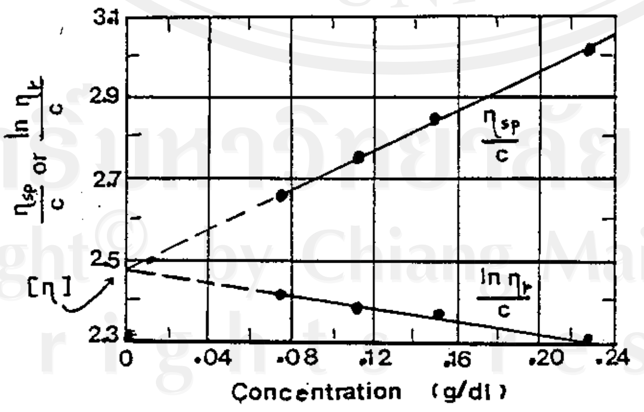

Fig. 3.52 : Reduced and inherent viscosity-concentration plots for a typical polymer sample.

Good straight line graphs are usually obtained when the concentrations of the solutions measured is not too large (i.e., < 1 % w/v), thus avoiding intermolecular forces and chain entanglement effects between polymer molecules of very high molecular weight.

(b) Solomon-Cuita One-Point Approximation Method

Measurement of the solution viscosity at only a single concentration can also enable calculation of the intrinsic viscosity, $[\eta]$, from the Solomon-Ciuta Equation [29].

$$[\eta] \quad = \quad [2\,(\eta_{sp} - \ln \eta_{rel})\,]^{1/2}\,/c \qquad (3.14)$$

This equation is obtained by combination of the previous equations (3.11), (3.12) and (3.13) followed by elimination of k' and k". However, this method is accurate only when it is already known that there is a good linear relationship between c and η_{sp}/c and/or $(\ln \eta_{rel})/c$.

3.7.3 Intrinsic Viscosity - Molecular Weight Relationship

The intrinsic viscosity, $[\eta]$, is related to the polymer molecular weight through the Mark-Houwink-Sakurada Equation [30,31,32].

$$[\eta] \quad = \quad K\overline{M}_v^{\,a} \qquad (3.15)$$

where: K and a are physical interaction constants for a given polymer in a given solvent at a given temperature, as listed for many combinations in the "Polymer Handbook" [33]. $\overline{M}_v$ is the so-called "viscosity-average molecular weight" of the polymer.

3.7.4 **Experimental Procedure**

Approximately 0.5 % w/v polymer solutions were accurately prepared using dimethyl sulfoxide (DMSO) as solvent. The solutions were prepared by heating to 150 °C under a dry nitrogen atmosphere. The flow-times, t and t_o, were then determined at 90 °C (± 0.1 °C) using a Schott-Gerate micro-Ubbelohde viscometer (type No. 531 03). In each case, particular care was taken to ensure that, following dissolution, the solution was not allowed to cool below the temperature at which the polymer would start to precipitate out of solution. Using the Solomon-Ciuta One-Point Approximation Method, the intrinsic viscosities, $[\eta]$, of each sample were calculated from the Solomon-Ciuta Equation (3.14). The results are given in Tables 3.31-3.32 for the PGA and P(GA-b-PEG) samples synthesized under the various conditions previously described.

Table 3.31 : Intrinsic viscosities of poly(glycolic acid) and P(GA-b-PEG 200): using aluminium triethyl as initiator.

Monomer Ratio (mole %) G : PEG 200	Temp. of Copolymerisation (°C)	Flow-time (sec)	η_{rel}	η_{sp}	$[\eta]$ (dl/g)
100 : 0	150	266.57	1.020	0.020	0.040
	180	269.47	1.031	0.031	0.061
	200	270.61	1.035	0.035	0.069
99 : 1	150	266.88	1.021	0.021	0.042
	180	268.38	1.027	0.027	0.054
	200	269.66	1.032	0.032	0.063
97 : 3	150	263.81	1.009	0.009	0.017
	180	264.25	1.012	0.021	0.024
	200	265.43	1.016	0.016	0.032
94 : 6	150	265.38	1.015	0.015	0.030
	180	263.67	1.009	0.009	0.018
	200	264.12	1.011	0.011	0.022
90 : 10	150	263.43	1.008	0.008	0.016
	180	264.54	1.012	0.012	0.024

Notes:

(1) t_o = flow-time of DMSO solvent at 90 °C = 261.35 sec.

(2) Flow-times, t and t_o, are the averages of at least 4 readings which agreed to within ± 0.2 % of their average value.

(3) Samples prepared as $0.50\ g.dl^{-1}$ solutions in DMSO.

(4) Viscosity terms calculated from:

Relative Viscosity = η_{rel} = t/t_o

Specific Viscosity = η_{sp} = η_{rel-1}

Intrinsic Viscosity = $[\eta]$ = $[2\ (\eta_{sp} - \ln \eta_{rel})]^{1/2}\ /c$

Table 3.32 : **Intrinsic viscosities of poly(glycolic acid) and P(GA-b-PEG 1500): using aluminium triethyl as initiator.**

Monomer Ratio (mole %) G : PEG 1500	Temp. of Copolymerisation (°C)	Flow-time (sec)	η_{rel}	η_{sp}	$[\eta]$ (dl/g)
100 : 0	150	266.57	1.020	0.020	0.040
	180	269.47	1.031	0.031	0.061
	200	270.66	1.035	0.035	0.069
99 : 1	150	264.67	1.013	0.013	0.026
	180	268.75	1.028	0.028	0.055
	200	269.25	1.030	0.030	0.059
97 : 3	150	264.60	1.012	0.012	0.023
	180	266.41	1.019	0.019	0.038
	200	282.91	1.082	0.082	0.160

From the data in Tables 3.31-3.32, the following conclusions can be drawn:

(1) Effect of Temperature

As the temperature of copolymerisation increased, the intrinsic viscosity of the polymer or copolymer increased. This is consistent with the earlier suggestion that higher temperatures enable the polymerisate to remain molten for a longer time during which the molecular weight can increase to a higher value before solidification occurs.

(2) Effect of Mole % PEG in Comonomer Feed

The general trend as the mole % PEG in the comonomer feed increased from 1-10 % was for the intrinsic viscosity of the copolymer to decrease. However, since the copolymer compositions are not exactly the same, their $[\eta]$ values will also vary slightly with chemical microstructure as well as molecular weight. In this case, the combined effects on $[\eta]$ of molecular weight and copolymer-solvent interactions in solution are impossible to separate.

(3) Effect of PEG Molecular Weight

On comparing the intrinsic viscosities of the P(GA-b-PEG 1500) copolymers with those of the P(GA-b-PEG 200) copolymers, no obvious conclusions can be drawn. Again, as in (2) above, the differing microstructures preclude comparisons of the $[\eta]$ on molecular weight grounds alone.

In general, however, taking the results in Tables 3.31 and 3.32 as a whole, it must be concluded that values of [η] of less than 0.1 indicate that the polymer/copolymer molecular weights are all relatively low, probably less than 5000. Unfortunately, absolute values of the molecular weights ($\bar{M}_v$) cannot be calculated due to the fact that the interaction constants K and a in the previous Mark-Houwink-Sakurada Equation (3.15) are not available in the literature for these speciality materials.

3.8 'In Vitro' Biodegradation of PGA and P(GA-b-PEG)

3.8.1 Apparatus

In this work, the apparatus used was as listed in the table below.

Table 3.33 : Apparatus used in 'in vitro' biodegradability experiments.

Apparatus	Company	Model
Vacuum Oven	Lab-line Instruments	3620-1
Incubator	Memmert	
pH-meter	Radiometer Copenhagen	PHM 61 a
Analytical Balance	Mettler	H 31 AR

3.8.2 Experimental Procedure

All glassware items were sterilized before use by steam autoclaving at 110°C for 20 mins. A phosphate buffer of physiological pH 7.40 prepared from a mixture of 0.2 M Na_2HPO_4 and 0.2 M $NaH_2PO_4.2H_2O$ was used as the immersion medium. Approximately 0.2 g of PGA and each of the copolymer samples were compressed into circular discs (diameter ≃ 10.1 mm, thickness ≃ 2 mm) using a pressure of

10 ton-ram area 33.18 cm^2 and re-weighed accurately. A total of 36 samples (6 sets of 6) were then immersed individually in 30 ml screw-top glass bottles, each containing 20 ml of the pH 7.40 phosphate buffer. The bottles were immediately placed in an incubator, thermostatically controlled at 37.0 ± 0.5 °C. At time intervals of 1 week, 6 bottles (1 from each set) were removed from the incubator and the samples filtered off, washed with distilled water, dried to constant weight in a vacuum oven at 60 °C, and their weights accurately recorded. The experiment lasted for a total of 6 weeks.

3.8.3 Weight Loss Calculations

The % weight retention for each sample was calculated as follows:

$$\% \text{ weight retention} = \frac{W_f \times 100\ \%}{W_o}$$

where:

W_o = initial weight of sample (before immersion)

W_f = final weight of sample (after immersion)

The % weight retentions and the pH changes in the phosphate buffer are shown in Tables 3.34-3.39 for each of the 6 sets of samples. To facilitate their comparison, the weight loss profiles are also plotted alongside each other in Fig. 3.53. Finally, the weight loss data for the PGA samples in Table 3.34 is compared in Table

3.40/Fig. 3.54, with that for commercial PGA ('Dexon') sutures obtained under the same conditions in a previous study [26].

Table 3.34 : Weights and % weight retentions of PGA, synthesized at 200 °C using aluminium triethyl as initiator, immersed in pH 7.40 phosphate buffer solution.

Time of Immersion (weeks)	Initial Weight ± 0.0001 (g)	Final Weight ± 0.0001 (g)	% Weight Retention ± 0.1	pH of phosphate buffer ± 0.01
1	0.2164	0.2004	92.6	7.40
2	0.2053	0.1355	66.0	7.40
3	0.2089	0.1266	60.6	7.40
4	0.2171	0.1266	58.3	7.40
5	0.2156	0.1244	57.7	7.35
6	0.1995	0.0984	49.3	7.00

Table 3.35 : Weights and % weight retentions of P(GA-b-PEG 200) 99:1, synthesized at 200 °C using aluminium triethyl as initiator, immersed in pH 7.40 phosphate buffer solution.

Time of Immersion (weeks)	Initial Weight ± 0.0001 (g)	Final Weight ± 0.0001 (g)	% Weight Retention ± 0.1	pH of phosphate buffer ± 0.01
1	0.2045	0.1878	91.8	7.40
2	0.2135	0.1399	65.5	7.40
3	0.2135	0.1295	60.7	7.40
4	0.2008	0.1190	59.3	7.35
5	0.2060	0.1175	57.0	7.30
6	0.2158	0.1040	48.2	7.10

Table 3.36 : Weights and % weight retentions of P(GA-b-PEG 200) 97:3, synthesized at 200 °C using aluminium triethyl as initiator, immersed in pH 7.40 phosphate buffer solution.

Time of Immersion (weeks)	Initial Weight ± 0.0001 (g)	Final Weight ± 0.0001 (g)	% Weight Retention ± 0.1	pH of phosphate buffer ± 0.01
1	0.2059	0.1834	89.1	7.40
2	0.2137	0.1521	71.2	7.40
3	0.2002	0.1288	64.3	7.40
4	0.1958	0.0989	50.5	7.30
5	0.1865	0.0848	45.5	7.30
6	0.2043	0.0823	40.3	7.15

Table 3.37 : Weights and % weight retentions of P(GA-b-PEG 200) 94:6, synthesized at 200 °C using aluminium triethyl as initiator, immersed in pH 7.40 phosphate buffer solution.

Time of Immersion (weeks)	Initial Weight ± 0.0001 (g)	Final Weight ± 0.0001 (g)	% Weight Retention ± 0.1	pH of phosphate buffer ± 0.01
1	0.2171	0.1945	89.6	7.40
2	0.2033	0.1209	59.5	7.40
3	0.2178	0.1232	56.6	7.40
4	0.1980	0.1009	51.0	7.30
5	0.2204	0.1064	48.3	7.30
6	0.2153	0.0863	40.1	7.20

Table 3.38 : Weights and % weight retentions of P(GA-b-PEG 200) 99:1, synthesized at 200 °C using stannous oxalate as initiator, immersed in pH 7.40 phosphate buffer solution.

Time of Immersion (weeks)	Initial Weight ± 0.0001 (g)	Final Weight ± 0.0001 (g)	% Weight Retention ± 0.1	pH of phosphate buffer ± 0.01
1	0.1919	0.1765	92.0	7.40
2	0.2112	0.1404	66.5	7.40
3	0.2059	0.1270	61.7	7.40
4	0.2023	0.1216	60.1	7.40
5	0.1993	0.1088	54.6	7.35
6	0.1954	-*	-	-

* error occured in the experiment

Table 3.39 : Weights and % weight retentions of P(GA-b-PEG 1500) 99:1, synthesized at 200 °C using aluminium triethyl as initiator, immersed in pH 7.40 phosphate buffer solution.

Time of Immersion (weeks)	Initial Weight ± 0.0001 (g)	Final Weight ± 0.0001 (g)	% Weight Retention ± 0.1	pH of phosphate buffer ± 0.01
1	0.2056	0.1859	90.4	7.40
2	0.2094	0.1355	64.7	7.40
3	0.2087	0.1275	61.1	7.40
4	0.1986	0.1108	55.8	7.40
5	0.2003	0.1104	55.1	7.40
6	0.2054	0.0965	47.0	7.20

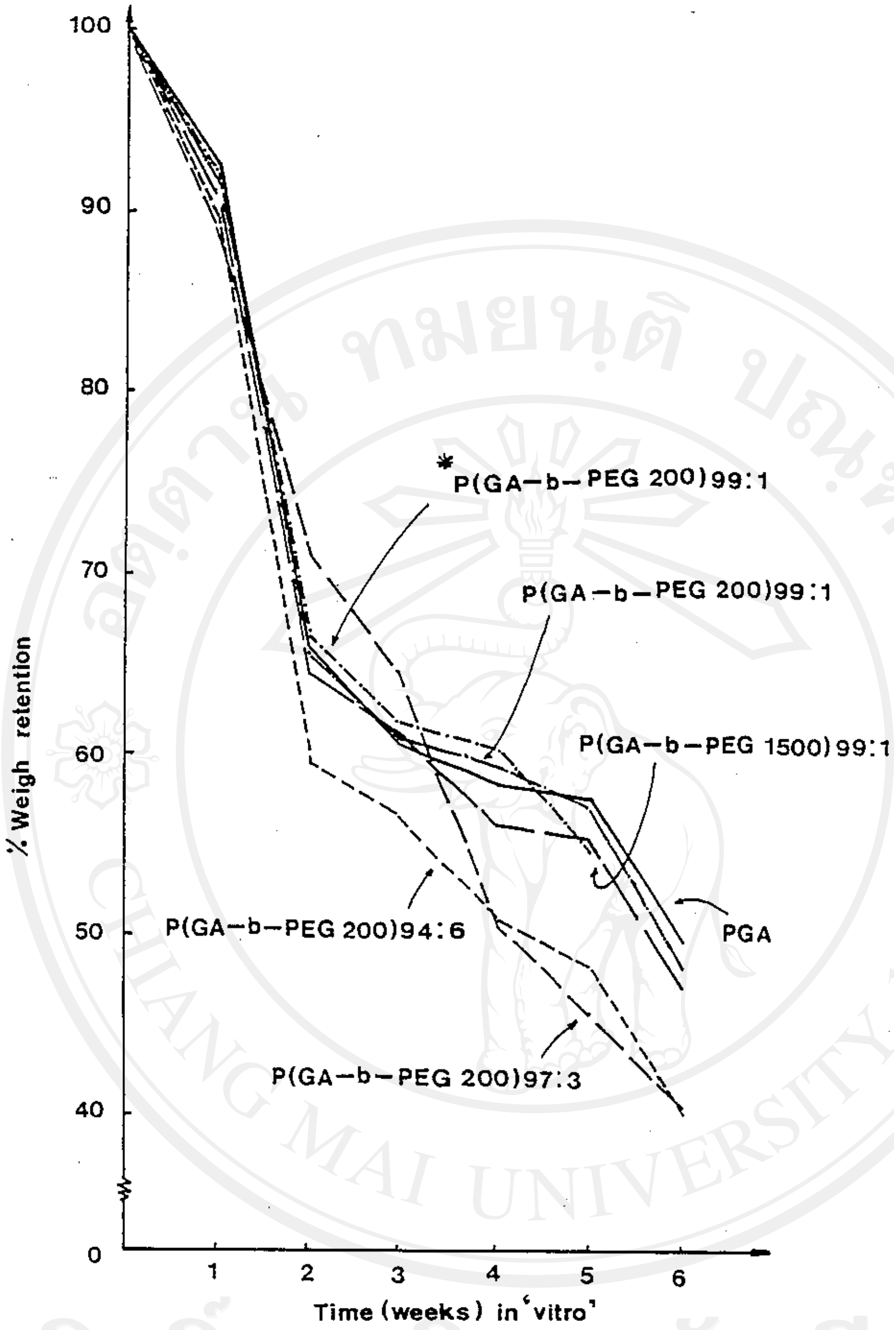

<u>Fig. 3.53</u> : Comparison of the 'in vitro' weight loss profiles of the PGA and various P(GA-b-PEG) samples studied in this work after immersion in pH 7.40 phosphate buffer solution at 37.0 °C for 6 weeks. (from the previous data in Tables 3.33-3.38)

* using stannous oxalate as initiator

Table 3.40 : Comparison of the % weight retentions of PGA from this study and commercial PGA ('Dexon') sutures from a previous study [26] after immersion in pH 7.40 phosphate buffer solution at 37 °C for 6 weeks.

Time of Immersion (weeks)	% Weight Retention (± 0.1)	
	PGA *	'Dexon' **
1	92.6	100.0
2	66.0	99.5
3	60.6	98.9
4	58.3	94.6
5	57.7	54.3
6	49.3	18.9

* PGA data taken from Table 3.33

** 'Dexon' data taken from reference [26]

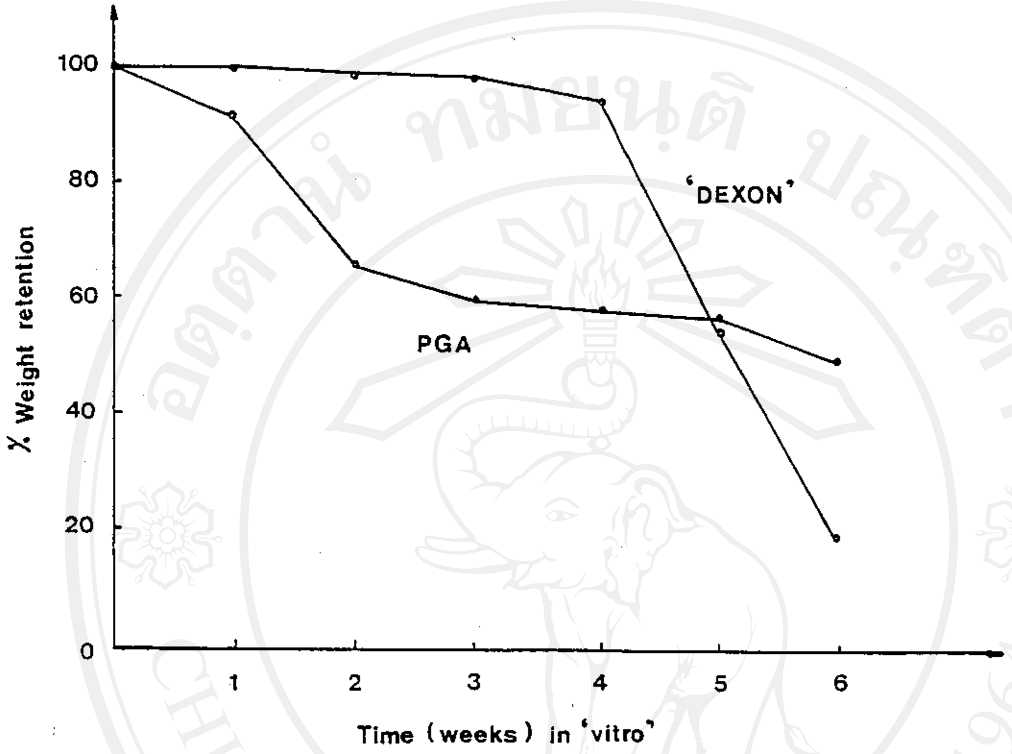

Fig. 3.54 : Comparison of the 'in vitro' weight loss profiles for the PGA synthesized in this work and commercial PGA ('Dexon') sutures from a previous study [26] after immersion in pH 7.40 phosphate buffer solution at 37°C for 6 weeks.

From the results shown in Tables 3.34-3.39 and Figs. 3.53-3.54, the following conclusions can be drawn regarding the 'in vitro' biodegradability of the polymers studied.

(1) Effect of PEG Content in Copolymer

From Fig. 3.53, as the PEG content in the copolymer increased, the rate of weight loss also increased. This finding is consistent with expectations since PEG is a water-soluble polymer whereas PGA is not. The presence of PEG blocks in the copolymer chain would therefore be expected to increase the rate of solubilization of the chain fragments following hydrolysis of the main PGA component. It can also be expected that the "soft segment" PEG blocks will increase the initial hydrophilicity of the copolymer and therefore the rate at which water molecules can adsorb at the surface and subsequently diffuse into the interior matrix. This combination of different biodegradation mechanisms within the same material-simple hydrolysis (for PGA) and solubilization (for PEG)-provides a potential means of controlling the rate of absorption in an 'in vivo' aqueous environment such as the extracellular fluid in the human body.

(2) Effect of PEG Molecular Weight

On comparing the two weight loss profiles for the P(GA-b-PEG 200) 200) 99:1 and P(GA-b-PEG 1500) 99:1 samples in Fig. 3.53, it is not surprising that the latter shows the slightly faster rate of weight loss. This is consistent with the previous arguments presented in (1). Since the PEG 1500 blocks are approximately 7.5 times longer than those in PEG 200, at the same mole % level they will exert a greater "flexibilizing effect" on the copolymer's matrix morphology. This, in turn, will enhance the contribution of the solubilization mechanism to the overall absorption process.

(3) Effect of Polymerisation Initiator

Comparison of the results for the two P(GA-b-PEG 200) 99:1 copolymers synthesized using different initiators, aluminium triethyl and stannous oxalate, as shown in Fig. 3.53, shows no clear inidication of any significant difference in their weight loss profiles. It must therefore be concluded that the nature of the initiator used is relatively uninfluential in determining the copolymer's subsequent biodegradability.

(4) Comparison of PGA synthesized in this work and commercial PGA ('Dexon') sutures [26]

Returning to Table 3.40/Fig. 3.54, there was very little weight loss in the 'Dexon' sutures during the first 2-3 weeks. This must have been because the low molecular weight chain fragments, formed as a result of hydrolysis, were still too large to diffuse out of the degrading matrix. This contrasts with the small water molecules which could easily diffuse in. Eventually, as the degradation products became small enough in size to diffuse out, the matrix became more porous, thus facilitating further diffusion in and out of water and products respectively. This resulted in an accelerating reduction in weight between 4-6 weeks. Finally, as bulk erosion reached an advanced stage, the suture fibres broke up into small fragments.

In contrast to this, weight loss in the PGA synthesized in this work occurred 'in vitro' within the first week of immersion.

The marked differences in the weight loss profiles, clearly shown in Fig. 3.54, must be due to physical factors since the PGA chemical structures are the same. These factors include:

(a) physical form/dimensions

'Dexon' sutures : braided multifilament fibres,
diam. ≃ 0.30 mm
synthesized PGA : compressed discs,
diam. ≃ 10.1 mm, thickness ≃ 2 mm

(b) polymer molecular weight

'Dexon' sutures : usually reported as $\overline{M}_n \simeq 20{,}000 - 50{,}000$
synthesized PGA : suspected as having $\overline{M}_n < 5000$

(c) polymer crystallinity (from DSC)

'Dexon' sutures : % crystallinity = 48 % [26]
synthesized PGA : % crystallinity = 46-48 %
[Table 3.25 /page 87]

From these differences in their physical properties, the much faster initial weight loss in the synthesized PGA can almost certainly be ascribed to its much lower molecular weight. This has the effect that the critical molecular weight level for diffusion of hydrolysis products out of the semi-crystalline matrix is reached much more quickly. It is probably also true that the synthesized PGA discs, made by simply compressing powdered samples, are initially more porous water than the melt spun fibres. However, by the end of the immersion period (weeks 5 and 6), the weight loss from the sutures had caught up with and surpassed that from the discs. The most likely explanation for this is that, once the sutures have reached the critical molecular weight level for diffusion out of products to occur (end of week 4), their higher surface area-to-bulk ratio enables continued hydrolysis and, hence, absorption to occur more rapidly. This effect is also aided by the onset of suture fragmentation which serves to increase the surface area of the degrading polymer still further.

In view of these differences in their weight loss profiles, it must be concluded that the results obtained for the compressed discs cannot be taken as a reliable guide to how the sutures would perform under the same 'in vitro' conditions. Biodegradability, under any conditions, is a property dependent not only on chemical structure but also on physical characteristics such as geometric configuration, surface-to-bulk ratio, macroporosity, polymer molecular weight and its distribution, and matrix morphology.

(5) Variation of Buffer pH with Time

Finally, from Tables 3.34-3.39, it can be seen that the initially adjusted pH of 7.40 of the phosphate buffer solution decreased during the final period of each experiment. This decrease in pH is undoubtedly caused by the release into solution of water-soluble acidic compounds formed as the products of the sample's hydrolytic breakdown. It therefore lends support to the simple hydrolysis mechanism of PGA biodegradation in an aqueous environment.